

Mimicking Insect Wings: The Roadmap to Bioinspiration

Jafar Hasan,[†] Anindo Roy,[‡] Kaushik Chatterjee,^{*,‡,†} and Prasad K. D. V. Yarlagadda^{*,†,†}

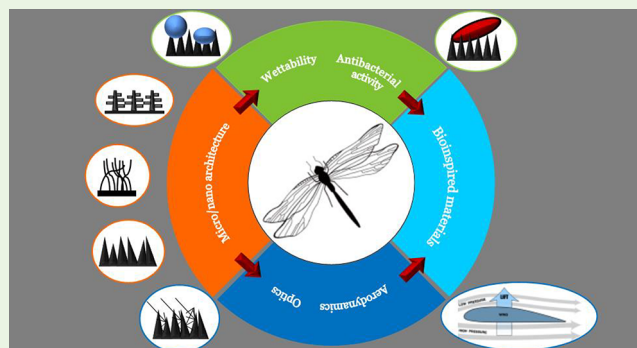
[†]Science and Engineering Faculty, Queensland University of Technology, 2 George Street, Brisbane, QLD 4001, Australia

[‡]Department of Materials Engineering, Indian Institute of Science, C. V. Raman Avenue, Bangalore 560 012, India

Supporting Information

ABSTRACT: Insect wings possess unique, multifaceted properties that have drawn increasing attention in recent times. They serve as an inspiration for engineering of materials with exquisite properties. The structure–function relationships of insect wings are yet to be documented in detail. In this review, we present a detailed understanding of the multifunctional properties of insect wings, including micro- and nanoscale architecture, material properties, aerodynamics, sensory perception, wettability, optics, and antibacterial activity, as investigated by biologists, physicists, and engineers. Several established modeling strategies and fabrication methods are reviewed to engender novel ideas for biomimetics in diverse areas.

KEYWORDS: biomimetics, insects, nanoscale architecture nanofabrication, surface science



INTRODUCTION

Engineers and scientists have been studying and developing devices by borrowing ideas from nature, especially insects, because of their diversity and abundance. Insects have evolved over millions of years to overcome complex challenges, resulting in some unique properties that have helped them survive. The origin of wings has been regarded as a key evolutionary change among insects, bats, birds, and the extinct pterosaurs, and wings contribute to the diversity of insects.¹ Insect wings are corrugated, membranous outgrowths from the exoskeletons and primarily help insects in flight.² Largely, insects possess two pairs of wings, namely, the forewings and hindwings. The wings are of different types, such as membranous, stiff, hard, scaled, and fringed with hairs. The appearance, color, and texture vary among different insects and within species. In addition to flight capability, these wings impart several other abilities to insects, such as protection, thermal sensing, sound generation, mating, visual recognition, hydrophobicity, and antibacterial activity. The aerodynamics and recently discovered bactericidal behavior of insect wings are some of the key properties that have been investigated extensively.

Insects have fascinated philosophers over the ages, as ancient Egyptians are known to have worshipped the dung beetle between 2500 and 1500 B.C. Some of the earliest documented works on insect wings were initiated in the early 19th century.^{3,4} The early investigations on insect wings were performed only by entomologists and curators. Now, however, many engineers and scientists have been attracted to the wonders of insect wings, especially the unique architecture at the micro- and nanoscale.

We analyzed the more than 2700 scientific publications (excluding book chapters and patents) on insect wings with applications in different areas over the last 7 years using the search engine tool Web of Science (Figure 1). The publications were categorized into 10 research areas, focusing on different categories of insect wing inspiration. The first area with the highest number of publications was flight movements and wing aerodynamics; the second area was bioinspiration and biomimetics; the third area focused on material properties, examining the stiffness and bending of insect wings; and the fourth area was antibacterial or bactericidal properties. Other areas such as wettability, sensing ability, and reflectivity have attracted increased interest, probably because of the recent progress in characterization techniques.

However, the number of publications does not represent the scientific impact of the specific areas. The Web of Science tool provides the h-index and average citation of all the searched publications. We performed a citation report analysis of the number of publications in the last 7 years on insect wings and subject areas (Figure S1), chronicled by their year of discovery. Although subject areas such as roughness, wettability, and superhydrophobicity had fewer publications, they had higher average citations. Notably, in the last 7 years, 19 papers covering topics of bacteria and insect wings have been cited at least 19 times (Figure S1).

The underlying theme of this review is bioinspiration from insect wings. Most studies have endeavored to understand

Received: February 12, 2019

Accepted: May 18, 2019

Published: May 22, 2019

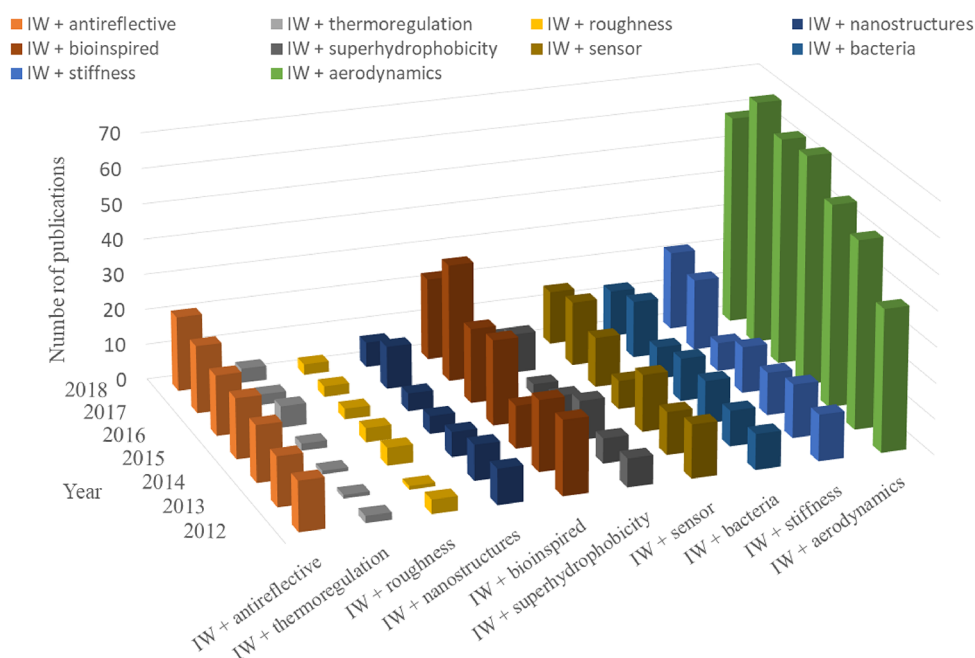


Figure 1. Skyscraper representation of the numbers of publications including insect wings (IW) in specific areas during the period 2012 to 2018. From the Web of Science search engine, the searches were done using keywords of insect wings and the specific areas. In the case of similar words, the OR function was used, such as IW + antireflection or IW + reflectivity and IW + bacteria or IW + antibacterial or IW + bactericidal. For simplicity, only one keyword is shown in the axis labels.

wing behavior and characteristics, whereas few have focused on actual mimicking vis-à-vis modeling and fabrication. From an engineering perspective, mimicking of the wing or rather its unique properties is as important as understanding the origin of the wing, evolutionary behavior, structure, or functions. Here an extensive review of the origin, evolution, structure, composition, classification, and multifunctional properties of insect wings is presented. The different multifunctional properties are grouped under bioinspiration, including micro- and nanoscale topography, material properties, aerodynamics, sensory perception, optics, wettability, and antibacterial activity. Following bioinspiration, biomimicry is discussed, with sections on modeling and simulation as well as fabrication. In the final section, future perspectives and concluding remarks are offered. There has been no single commentary, analysis, or review of the cumulative work done on the unique and attractive properties of insect wings, and this review is an attempt to address that need.

■ ORIGIN AND EVOLUTION OF WINGS

The origin of insect wings has been debated for centuries, as contrasting theories based on the study of fossils have been put forth. The problem lies in the absence of fossils detailing the transition between nonwinged and winged insects.⁵ Primarily, two theories have been proposed by biologists: the tergal or paranotal hypothesis and the pleural or gill hypothesis. In the paranotal hypothesis, which was more accepted during the 20th century,⁶ the wings extended from the dorsal body wall or the paranotal lobes to help insects initially in gliding followed by flying in order to avoid falling from a height.^{7,8} In the gill hypothesis, the wings extended from the leg segments and the branches or exites, which helped the wings to show musculature and articulation.^{9,10} The debate over the two hypotheses is essentially based on the possibility that insect wings developed either from pre-existing structures or as new

structures. Gegenbaur¹¹ and Müller¹² separately proposed in the 1870s that insect wings originated from tracheal gills and tergal lobes, respectively.⁶ Many scientists supported the gill theory, or its variation known as the pleural appendage theory, in the latter half of the 20th century.⁶ However, in the absence of transition fossils, neither of the theories can be rejected. In 1997, the gill hypothesis again gained wide acceptance as a result of the innovative work on development genetics by Averof and Cohen.¹³ A dual or combined hypothesis proposing the hybrid development of wings from composite structures was put forth in 2010;¹⁴ it has been confirmed by several studies, and its acceptance is on the rise.¹⁵ The contributions of different tissues and body parts to the origin of insect wings vary with the theory, and their specific contributions to the origination remain an active subject of investigation.^{5,16,17}

■ CLASSIFICATION, STRUCTURE, AND COMPOSITION

According to the International Commission on Zoological Nomenclature (ICZN), living organisms have a specific taxon classification: kingdom, phylum, subphylum, superclass, epiclass, class, subclass, superorder, order, suborder, superfamily, family, subfamily, tribe, genus, and species.¹⁸ Insects belong to the animal kingdom, arthropoda phylum, and insecta class. The identification of insects is a complex and daunting task because of their diversity. The number of described species of insects is close to 1.5 million, whereas the mean total estimate is around 5.5 million.¹⁹ Generally, insects can be classified into two major subclasses, namely, apterygota (nonwinged) and pterygota (winged). Most species come under the subclass pterygota, which is further divided into palaeoptera (primitive wing) and neoptera (new wing). The primitive insects that belong to palaeoptera, such as dragonflies, damselflies, and mayflies, have nonfolding wings,



Figure 2. Photographs of (A) dragonfly, (B) butterfly, (C) hoverfly, and (D) damselfly, displaying the diversity in wing design. Photographs courtesy of (A) Lars Kristensen, (B, C) Enguerrand Masse Apere, and (D) Rikuto Kuraishi.

whereas the neoptera insects can fold their wings back. Insects under neoptera are further subdivided into exopterygota and endopterygota. Exopterygota species undergo moderate changes during development, whereas the endopterygota species undergo complete changes during development or undergo complete metamorphosis, which is found in insects such as beetles, butterflies, ants, and moths.²⁰

The identification of insect wings can be done utilizing different wing characteristics, in which a reasonable number of factors (or keys) can be taken into account.²¹ With the help of DNA barcoding, available taxonomies, and computer software such as Lucid Central, identification of insects may be accurately performed in the future. The venation of wings has been used to identify species. The recognition of features of the venation of insect wings was first generalized by Comstock and Needham in 1898.²² This was further developed such that a common nomenclature of veins and branches exists in numerous wings among millions of insects.^{23,24} There are six to eight major longitudinal veins, including costal (C), subcostal (Sc), radial (R), medial (M), cubital (Cu), anal (A), and jugal (J) veins.²⁵ Furthermore, the wings have several fields, joints, cross-veins, flexion lines, joint lines, branches, and sub-branches. The major veins separate into anterior (convex) and posterior (concave) sectors; the anterior sectors are present on the upper layer of the wings, whereas the posterior sectors are present on the lower layer. The cross-veins, which are small veins that connect the longitudinal veins, are more variable than the longitudinal veins and provide information for species characterization. The topic of venation among insects has been extensively compiled elsewhere.²⁶

Insect wings have two membranes supported by a rigid network of veins. The wings are made up of cuticle, which has different functions but primarily acts as an exoskeleton that provides shape and support to structures such as wings.^{27,28} The cuticle in various layers of the wings varies in thickness and is composed of various substances such as chitin and long-chain hydrocarbons among orders and species of insects. The

outermost layer of the cuticle is epicuticle; it is very thin and is further divided into outer, meso-, and inner epicuticle.²⁹ The composition of the outermost epicuticle layer in several species of dragonflies has recently been characterized.^{30,31} In dragonfly wings, the outer layer is made up of long-chain aliphatic hydrocarbons and fatty acids such as palmitic acid and stearic acid. The next layer, procuticle, is composed of chitin microfibers and proteins and is further divided into a hard exocuticle and a soft endocuticle. The hardness of the exocuticle layer is attributed to the cross-linking of quinone compounds with individual protein molecules^{27,32} through a chemical process called sclerotization. In the endocuticle, an elastic protein called resilin is also present that makes the layer softer.^{33,34} The presence of resilin in many insect wings, such as those of beetles, dragonflies, and damselflies, provides an elastic property that imparts higher stiffness and lower deformability to the wings against aerodynamic loads.^{35–37} Moreover, resilin assists in the folding of wings in order to circumvent any damage during flight.³⁵ The folding direction is determined by the distribution of resilin in the radiating and intercalary veins.³⁸ In the different wing layers, the cuticle possesses different compositions, orders, and thicknesses that vary according to the insect species.

The wings have different phenotypic characteristics such as size, shape, color, and veins (Figure 2). Wing growth is dependent on a point in time when the insect body stops growing.³⁹ The wing size and shape of the insect may vary as a result of migration and mate guarding.⁴⁰ Some insects may have scales, such as those found on the wings of butterflies and moths. The wing coloration arises from pigmented patterns, melanin production, eyespot concentric rings, or structural colors.^{41,42}

■ BIOINSPIRATION

Micro- and Nanoarchitecture. To the best of our knowledge, Stainton's description of "small spots" in 1859 is one of the earliest reports where microstructures on the wings were observed.⁴³ However, there were earlier endeavors on

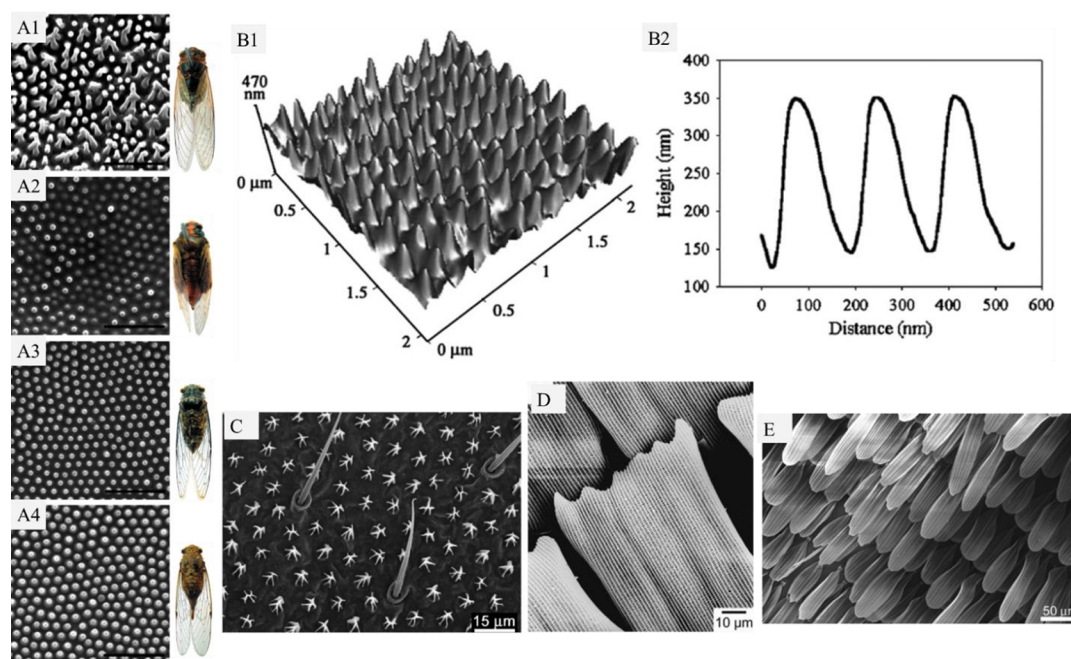


Figure 3. (A1–A4) SEM images and corresponding photographs of the cicada wings of *Chremistica maculate*, *Mogannia conica*, *Meimuna microdon*, and *Terpnosia jinpingensis*, respectively (scale bars = 1 μm). (B1) AFM image and (B2) height profile of the nanopyllars of cicada (*Psaltoda claripennis*) wing. (C–E) SEM images of the micro- and nanostructures on the wings of (C) *Nasutiterems walkeri* termite, (D) *Speyeria aglaja* butterfly, and (E) *Prasinocyma albicosta* moth. Reproduced with permission from (A) ref 50, (B) ref 55, (C) ref 53, (D) ref 253, and (E) ref 254. Copyright 2009 The Company of Biologists, 2008 The Biophysical Society, 2010 American Chemical Society, 2014 Science China Press, and 2011 Taylor & Francis, respectively.

insect wings where the necessity for a higher microscope power for examination was mentioned.⁴⁴ The small-scale features, initially described as microsculptures on the wings,^{45–48} are now termed micro- or nanopatterns, -features, -structures, or -spikes/pillars. The micro- and nanoscale architecture, which is typically observed with scanning electron microscopy (SEM) or atomic force microscopy (AFM), describes the surface morphology of the insect wing membrane (Figure 3 and Table S1). Some of the recently studied nanoscale features of the cicada and dragonfly wings have been characterized as nanopyllars (Figure 3A–C). Nanopyllars are erect rod-shaped pillars that are consistently present on both the dorsal and ventral sides of the wing surface, including the veins; their dimensions vary among species and orders of insects. In cicada wings, the nanopyllars are hexagonally packed, and the topography arrangement varies among species. The height of each nanopyllar varies from 150 to 450 nm, the diameter varies from 80 to 210 nm, and the center-to-center spacing (pitch) varies from 45 to 250 nm across the cicada species tested to date.^{49,50} In dragonfly wings, randomly oriented nanopyllars are found, some of which are connected to each other at the top. There have been variations reported within different regions of dragonfly (*Sympetrum vulgatum*) wings, where the diameter varies between ~ 80 to 200 nm.⁵¹ In statistical testing of the variance among different species of dragonflies, 77% proportion of variation in nanopyllar density, 34% proportion of variation in nanopyllar height, and 25% proportion of variation in nanopyllar diameter have been reported.⁵² Therefore, it is understood that the surface architecture varies largely among species and orders of insects.

It has been postulated that the variation in nanoarchitecture is probably due to differences in taxon, geography, habitat, migration, and foraging characteristics.⁵² Recently, the group

of Gregory and Jolanta Watson has done work on the characterization of micro- and nanoarchitecture and the related multifunctional behavior of insect wings.^{50,53–59} The group has categorized the micro- and nanoarchitectures of insect cuticles into seven groups, which include simple microstructures, simple nanostructures, complex geometric microstructures, complex geometric nanostructures, scales, hairs/setae, and hierarchical structuring.⁵⁷ The presence of architecture at different length scales obviously assists insect wings with various properties and functions, as reviewed in the following sections.

Material Properties. To counter the threats and stresses encountered by flying insects, wings have evolved biomechanical strategies. During the lifetime of the insect, wings undergo high mechanical stresses and millions of cycles of loading but still maintain excellent resistance to fatigue and fracture.^{28,60,61} It has been shown that veins reduce crack propagation.⁶⁰ Moreover, the fracture toughness of wings is enhanced by 50% by the presence of cross-veins.⁶¹ Similar to the role of grain boundaries in metals that act as barriers for crack propagation, wings use veins to stop crack propagation; this eventually provides them with enhanced biomechanical properties and scope for inspiration. The wear and tear of wings due to collisions, age, and forage have been known to affect performance and functions such as maneuverability, hunting, and predator evasion.⁶² Recently, the wings of the wasp and bumblebee were experimentally subjected to wear, and their response to collision damage was tested.⁶³ It was found that the two insects exhibit similar behaviors but have different wing venations. The “costal break”, which is a flexible resilin joint found on the leading edge of wings of many insects, such as wasps, is primarily responsible for mitigating collision damage. However, the costal break is absent in less-rigid

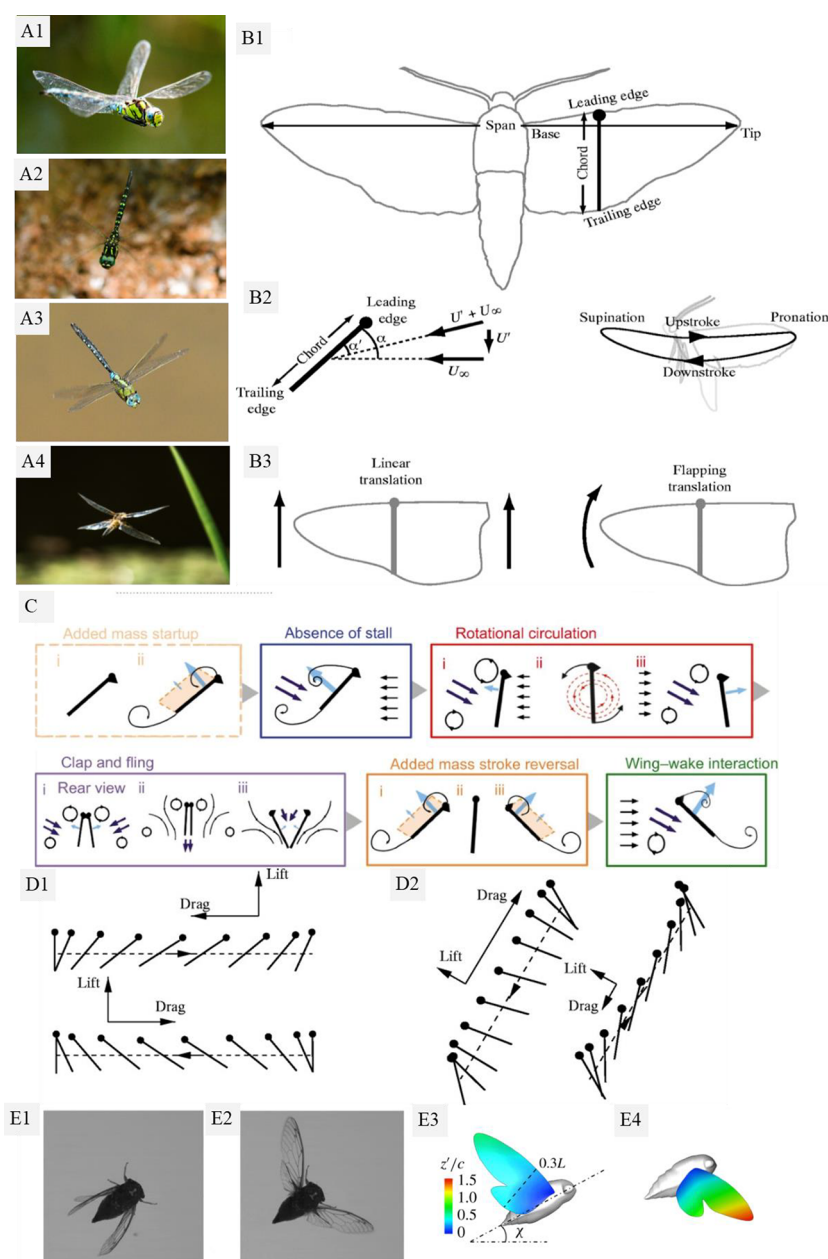


Figure 4. (A1–A4) Photographs of dragonflies depicting flight maneuvers. (B1–B3) Schematic of an insect wing leading edge, chord, trailing edge, and various strokes used in various phases of insect kinematics. In B2, U_∞ is the free stream velocity, U' is the downwash velocity, α is the geometric angle of attack that the wing section makes with the free stream velocity, and α' is the aerodynamic angle of attack, which is the angle between the wing section and the free stream velocity deflected as a result of downwash. (C) Schematics of various complex aerodynamic mechanisms discussed in *Aerodynamics*. (D1, D2) Horizontal and inclined hovering of various insects. (E1–E4) Photos and model images representing downstroke and upstroke motions of a cicada. Reproduced with permission from (B) ref 78, (C) ref 71, (D) ref 211, and (E) ref 255. Copyright 2003, 2016, and 2004 The Company of Biologists and 2016 Cambridge University Press, respectively. Photographs courtesy of (A1, A4) Lars Kristensen and (A2, A3) Rikuto Kuraishi.

bumblebee wings, which have a different configuration of veins and may not require buckling during collisions.

Aerodynamics. Insects were the first organisms that developed flight. Many of the maneuvers of flying insects demonstrate their superior flight performances.⁶⁴ Because of the small size and high frequency of the wings, insect flight is still not completely understood. The configuration of muscles and wings gives rise to direct and indirect flight mechanisms. In direct flight, the muscles of the wings are hinged to the base directly; this is found in primitive four-winged insects such as dragonflies and mayflies. Two groups of muscles, the

depressors and the elevators, are known to help these insects during downstrokes and upstrokes in direct flight.⁶⁵ In all other insects, the wing movement is determined by deformation of the thorax, which defines the indirect flight mechanism.⁶⁵ Here the vertical and longitudinal muscles govern the movements. When the vertical muscle is contracted, the thorax oscillates, giving rise to an upstroke.⁶⁶ Similarly, the longitudinal muscle is contracted to shorten the thorax in a downstroke movement.⁶⁶ The upward and downward wing movements are facilitated by the indirect vertical and longitudinal muscles.

In addition to normal flying patterns, some insects have the ability to hover, fly backward or sideways, take off backward, and land inverted.^{67,68} Wing motion has two translational phases, upstroke and downstroke, and two rotational phases, pronation and supination.⁶⁹ The highly improbable vertical lift produced by lightweight insects has been a topic of extensive research.^{69–71} There are various mechanisms responsible for the enhanced aerodynamics of insects (Figure 4), of which some are reported⁶⁹ to be distinct yet interactive: (i) In delayed stall, before the lift, the insect wing flaps at a large angle of attack, forming a vortex on the leading edge of the wing. If the vortex were to leave the leading edge, then the lift would be lost and the wing would be stalled (stop “lifting”). However, the stall is delayed in an entire downstroke or upstroke, and the leading-edge vortex is maintained on the wings.^{70–74} (ii) In rotational circulation, the mechanism is based on the rotation of wings, which facilitates circulation to generate an upward force. (iii) In wake capture, or wing–wake interaction, immediately following stroke reversal, the wing sheds leading- and trailing-edge vortices, which helps in generating force (Figure 4). The flow generated by one stroke can enhance the velocity at the start of the next stroke, thereby increasing the produced force, which cannot be explained by the translational force alone.⁶⁹ In the wake capture hypothesis, it is predicted that the wing must continue to generate force even after coming to a complete stop at the end of a half stroke; this was tested by Dickinson et al.⁶⁹ There are numerous other mechanisms, principles, and modeling methods that aid in better understanding the aerodynamic behavior of insect wings such as clap and fling,^{75,76} added mass,^{77–79} and evasion of the Wagner effect.^{80,81} Several mechanisms that assist in high-frequency flapping have also been postulated, including rotational drag and trailing-edge vortex.^{82,83}

The structure of insect wings has also been studied in relation to aerodynamic functions. For example, the nodus (a specialized wing part) contains resilin, which helps the wing to deform without breaking during flight in dragonflies.⁸⁴ However, to save itself from excessive deformation, the nodus can also restrain its displacement in the form of a one-way locking mechanism. The nodus is important in the design of bioinspired flying devices.⁸⁵ In the locust, automatic cambering in the hind wings during lift gives it the umbrella effect operating in the vannus.⁸⁶ Similar to the spokes and curves during opening of an umbrella, the vannus margin becomes stiff when it is pulled inward during the stretching of the wing to a certain point.⁸⁷ The recent efforts to understand the aerodynamics of insect wings have been such that the expedition has also moved toward enhancement of flying efficiencies.⁸⁸ With the advent of advanced electronics and/or robotics, insect wings are now inspiring the design of flying robots or drones.^{89–93}

Sensory Perception. Insects contain a variety of sensors on the antennae and other body parts. To date, however, there are only two known sensors associated with insect wings, namely, gyroscopic and thermoregulatory perceptions. The mechanosensory structures or mechanoreceptors that are present on the halteres as well as the wing cuticle assist the insects in flight maneuvers.^{94–97} The halteres function as vibrating gyroscopic sensors under the Coriolis effect. The receptors or structures, known as campaniform sensilla, are observed to assist as sensors providing feedback regarding body rotations.^{98–100} It has been hypothesized that insect

wings also assist in thermoregulation, although this is a secondary function, as temperature control is primarily performed by the main body.^{101–103} Similarly, the wings assist in other functions such as mating, defense, territorial attack, and camouflage.¹⁰¹ Inspired by the wings of the glasswing butterfly, a recent study demonstrated that nanostructured surfaces have the potential to be used as intraocular pressure (IOP) sensors in medical devices with multifunctional properties.¹⁰⁴ Apart from wings, insects use other multisensory organs such as antennae for sensory perception (smell, sound, and humidity).^{105,106} During flight, the antennae also provide orientation, maneuverability, stability, and speed control.^{107,108}

Wettability. The wettability of solid surfaces by liquids is a fundamental property of materials that plays a crucial role in a wide range of applications such as optics,¹⁰⁹ biomedical implants,¹¹⁰ food packaging,¹¹¹ and industrial processes, including oil recovery.¹¹² In nature, many biological materials—including the surfaces of insect wings—are known to exhibit unusual surface wettability. The wettabilities of numerous insect wings have been estimated by measuring the contact angle of droplets on the wing surfaces (Table S1). It was concluded that the nonwetting or ultrahydrophobic property is related to the presence of evolutionarily developed fine structures on the wing surfaces. If the static water contact angle is greater than 150° and the contact angle hysteresis is less than 10°, the surfaces are called superhydrophobic self-cleaning surfaces. On the wings of some insects, a water droplet rolls away by collecting surface dust particles, thereby making the wing surfaces self-cleaning, a property also found in lotus leaves and termed the “lotus effect”. Barthlott and colleagues examined the wing microstructures on 97 insect species and correlated a relationship among surface structure, wettability, and effects on contamination.¹¹³ They also developed a correlation between wettability and SM index (the quotient of wing surface area to body mass); it was found that insects with high SM index or large wings have more nonwetable surfaces than those with low SM index or small wings.

Various wettability models, such as the Cassie–Baxter and Wenzel models,^{114,115} have been proposed to rationalize the superhydrophobic behavior of a substrate due to topography. In superhydrophobic insect wings, there is a transition from the Wenzel state to the Cassie–Baxter state due to the presence of dual-scale roughness or architecture.¹¹⁶ Insect wings such as those of cicadas,^{50,59,117} damselflies,¹¹⁸ butterflies,¹¹⁹ termites,^{53,120} beetles,¹²¹ crane flies,¹²² and lacewings¹²³ demonstrate superhydrophobic behavior. The superhydrophobic feature is due to micro- and nanoscale structures that also make the wings capable of maintaining a contaminant-free surface despite the presence of abundant contaminants in their surrounding environments. Because of the arrangement of micro- and nanostructures, the wings of butterflies possess directional wetting or anisotropic wetting, which can serve as an inspiration for the transport of liquids in microfluidic channels or devices.^{124,125} Insect wings have been used as model substrates to design several functional surfaces with special wettability^{126–129} for practical applications such as self-cleaning windows, windshields, exterior paints for buildings and navigation ships, utensils, roof tiles, textiles, and reduction of drag in fluid flow.

Optics. Through evolution, insects have developed unique light manipulation strategies that rely on intriguing combinations of a broad range of optical effects, including broad-angle

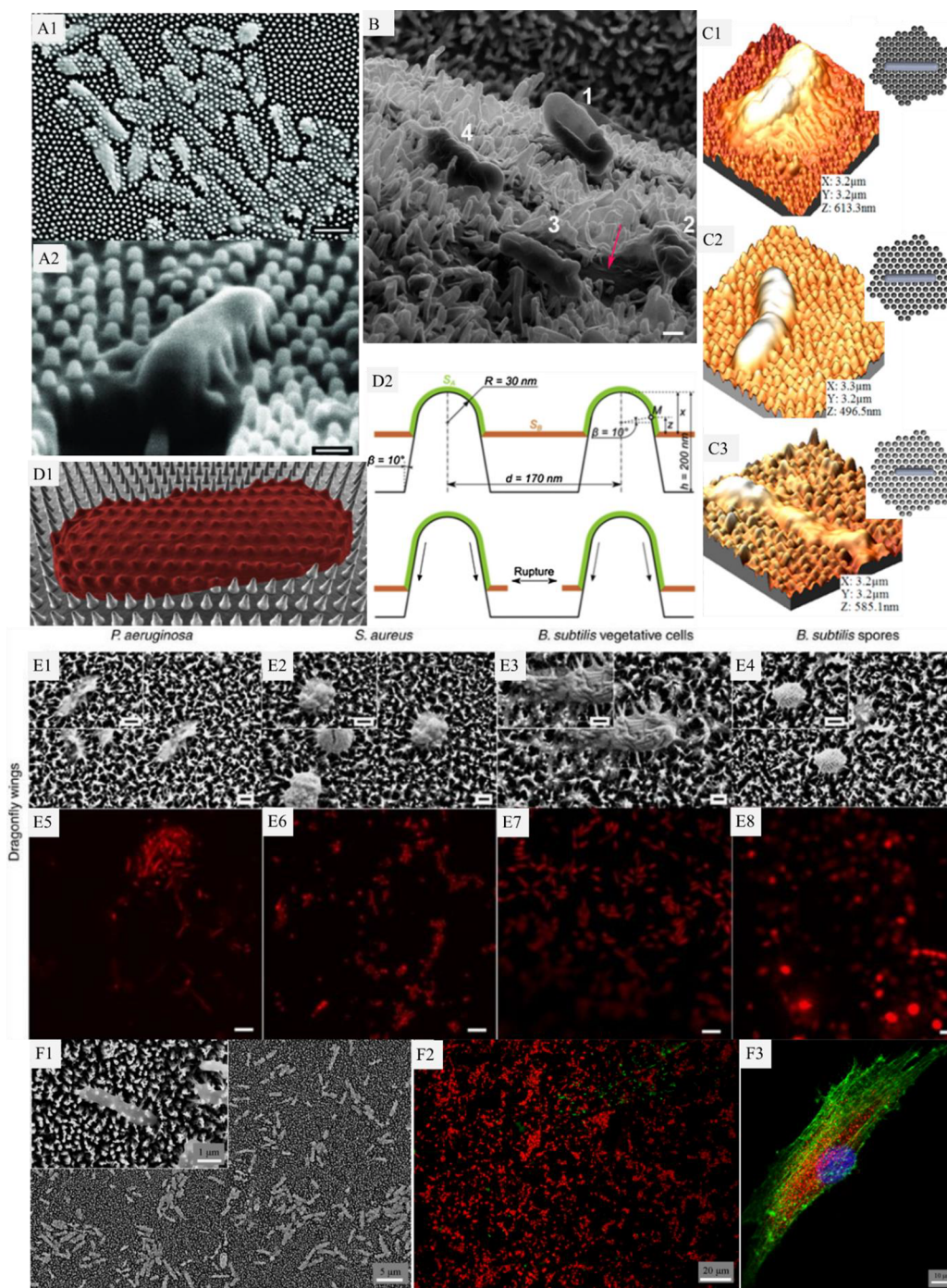


Figure 5. (A1, A2) SEM images showing the bactericidal effect of cicada wing nanopillars against *Pseudomonas aeruginosa* cells (scale bars = 1 μm (A1), 200 nm (A2)). The bacteria cells settle down at the wing surface, where they appear to be lysed by the nanopillar architecture. (B) Different *Escherichia coli* cells are affected upon contact with the dragonfly wing nanopillars (scale bar = 200 nm). The nanopillars on dragonfly wings are not patterned like those on cicada wings, but the effect is similar. (C1–C3) AFM images and corresponding schematics of a single bacterial cell interacting with three different species of cicada wing nanopillars. The nanopillars are seen to have different nanotopographies, and their effect on the bactericidal activity was studied. (D1, D2) Schematic and geometric model representation of the bacterial cell interaction with the nanopillars of the cicada wings. The top figure shows the bacterial cell being stretched by the nanopillar, which is represented by green color, whereas the stretched part of the cell membrane is suspended between the nanopillars, which is represented by the orange color. The bottom figure shows the ruptured cell, where the cell has reached its limit to stretch. (E1–E4) SEM and (E5–E8) fluorescence microscopy images of different bacterial strains on the dragonfly wing surface (scale bars = 200 nm (E1–E4), 5 μm (E5–E8)). (F1) SEM and (F2) fluorescence microscopy images of *E. coli* cells on a wing-inspired nanostructured titanium surface (scale bars = 5 μm (F1), 1 μm (F1 inset), 20 μm (F2)). The fluorescently labeled cells are red, indicating that the cells are nonviable or damaged. (F3) Image of a human mesenchymal stem cell attached to the nanostructured titanium surface (scale bar = 10 μm), depicting cytocompatibility for orthopedic applications. The cell is stained for parts of the cell indicating adhesion, such as paxilin (red), actin filaments (green), and nucleus (blue). Reproduced with permission from (A) ref 231, (B) ref 176, (C) ref 49, (D) ref 179, (E) ref 186, and (F) ref 185. Copyright 2012 Wiley-VCH, 2017 and 2016 American Chemical Society, 2013 The Biophysical Society, 2013 Macmillan Publishers Ltd., and the authors of ref 185, respectively.

structural color,¹³⁰ color mixing,¹³¹ polarization,¹³² antireflection,¹³³ iridescence,¹³⁴ ultrablackness,¹³⁵ and ultrawhiteness,¹³⁶ generated by materials with sophisticated multiscale hierarchical structural arrangements. Such optical effects serve important roles in camouflage, conspecific and heterospecific signaling, and so forth. Apart from coloration due to pigmentation, these features on the wing surface are responsible for coherent and incoherent light scattering. The former owes its origin to the periodic regularities of microstructure in the surface layer, which are on the order of the wavelength of light. In a unique phenomenon called iridescence, observed on the wings of many butterflies and moths, the perceived color depends on the angle of observation. The structures can be thin films,¹³⁷ multilayers incorporated into the scale ridging or scale body,^{137,138} or three-dimensional sculptures called photonic crystals.^{55,138,139} By the use of the optical principles underlying these natural systems, possible applications in security labeling and anticounterfeiting,^{140–142} photovoltaic systems such as solar panels,^{133,135,143–147} colorimetric sensing,^{148–151} iridescent textile apparel and aesthetic surfaces,^{152,153} water quality monitoring,^{154,155} and others^{154,156–158} have been suggested. In many cases, optical properties arise solely due to pigmentation or because of a synergistic effect of the nanostructures and pigments present. Incoherent scattering results when light encounters random irregularities with separations larger than the coherence length of light; this may cause Rayleigh or Tyndall scattering.¹⁵⁹

The colors of butterfly wings are produced from microscopic scales, consisting of upper and lower lamina linked together by trabeculae.¹⁶⁰ Embedded within these scales are melanin pigments that create black and brown undertones. As light scatters within a scale's crystalline structure, it produces iridescent blues, greens, and reds. The most vividly studied butterflies are those belonging to the *Morpho* genus.^{139,149,160,161} The lustrous blue characteristic of butterflies is due to the constructive interference of light by exquisite “Christmas-tree-like” photonic nanostructures present on their scales, even though the cuticle protein that constitutes these structures is almost transparent.¹⁶² These nanostructures possess alternating lamellae of materials having high and low refractive indices, producing the blue color; vertical and horizontal offsets exist between neighboring “trees” that eliminate interference among ridges, resulting in diffuse and broad reflection of a uniform color.¹⁶³ Contrarily, the wings of *Papilio palinurus*, also possessing multilayers, exhibit color mixing because of the juxtaposition of light reflected from the flat and concave regions of the wing, thus flaunting an angle-dependent change in color appearance.¹³¹ Yet another species (*Pierella luna*) shows an intriguing rainbow iridescence effect in which the sequence of colors is reversed (red to blue). This exquisite phenomenon occurs through decomposition of white light by redirecting visible colors into specific emergence angles using a diffraction grating.¹⁶⁴ Fascinated by this broad range of optical properties incorporated into a single surface, researchers are trying to reproduce similar structures artificially.^{157,163}

Many insects with flight-dependent lifestyles have optically transparent wings of 1 to 2 μm ultrathin membranes of chitin. In order to veil glare and reduce thin-film interference,¹⁶⁵ some insects have developed two-dimensional (2D) photonic nanostructures on their wing surfaces. Cicada wings have been characterized by a highly ordered nanonipple array

structure, which plays a dynamic role in reducing reflection of light over a broad spectral range of wavelengths.^{49,144} The nanoscale structures introduce a gradient in the refractive index between air and the material by presenting a “material–air composite”, thereby reducing the Fresnel reflection and consequently increasing the amount of incident light transmitted across the wings.^{143,147} The glasswing butterfly (*Greta oto*) also has an array of small nanopillars on its wings, imparting omnidirectional antireflection behavior.¹⁶⁶ Sun et al. studied the dependence of optical reflectivity and wettability on the surface topography of 32 species of cicada wing membranes¹⁴⁴ and discovered a near-linear relationship decrease in protuberance height and a resulting increase in reflectance intensity. Nanoscale antireflective architecture has also been found in wing scales of *Papilio ulysses* and *Troides aeacus* butterflies.^{142,167} The latter was found to have a combination of structures of ridges and grooves responsible for light trapping. Some advanced nanofabrication techniques to imitate the antireflective surface (ARS) of cicada wings have been developed, such as soft imprint lithography, reactive ion etching, sol–gel process, microinjection compression molding, chemical etching, and replica molding.^{146,147,168,169} ARSs have the potential to maximize the performance of solar cells, light sensors, and high-contrast and stealth surfaces. A detailed review of the mathematical principles and manufacturing strategies of ARSs has been published.¹⁴³ Cicada wings have also been suggested for direct use as efficient surface-enhanced Raman spectroscopy (SERS) substrates.¹⁷⁰ The wings of the dragonfly¹⁷¹ and hawkmoth¹⁷² have been studied; however, they are yet to be replicated artificially. The wings of dragonfly *Aeshna cyanea* were found to be coated both ventrally and dorsally with a nanostructured wax coating that is associated with a wavelength-dependent and complex refractive index of 1.38 to 1.40 and has optical absorbance an order of magnitude smaller than that of butterflies, accounting for the transparency.¹⁷³

Antibacterial Activity. Antimicrobial surfaces have the ability to repel microbial cells, mitigate their attachment, or kill them upon surface adhesion.^{174–176} The presence of nanoscale architecture on insect wings renders them antimicrobial by killing the microbe upon contact (Figure 5).^{177,178} Ivanova et al. first reported that the wing surface of the *Psaltoda claripennis* cicada, consisting of robust hexagonal arrays of spherically capped conical nanopillars, is bactericidal rather than antibiofouling, i.e., it kills bacteria rather than merely preventing attachment or halting biofilm formation.^{174,178} They proposed a contact killing mechanism wherein the nanopillars present on the wing penetrate bacterial cells, causing them to die with no apparent role of surface chemistry.¹⁷⁸ Mathematical calculations showed that adsorption of the bacterial cell membrane on the pattern of the cicada wing surface leads to a drastic increase in the total area accompanied by stretching of the membrane; this in turn leads to irreversible membrane rupture and death of bacteria.¹⁷⁹ A detailed study was published subsequently by Hasan et al.¹⁷⁷ in which the bactericidal activity of cicada wings was tested against seven bacterial species with variable properties covering every combination of cell morphology (rod-shaped and spherical) and cell wall structure (Gram-positive and Gram-negative bacteria). It was revealed that the surface efficacy is independent of cell shape but depends on the bacterial strain.¹⁷⁷ Thus, Gram-positive bacterial strains, which have a thicker and more rigid cell membrane (because of the presence of peptidoglycan in higher

Table 1. Bactericidal Activity of Investigated Insect Wings

| year | insect | species | geometry | surface architecture | bactericidal activity | ref(s) |
|------|-----------|---|---------------------|--|--|----------|
| 2012 | cicada | <i>Psaltoda claripennis</i> | conical nanopillars | height: 200 nm diameter: 100 nm (base), 60 nm (cap) spacing: 170 nm | First reported mechanobactericidal surface. Tested against <i>Pseudomonas aeruginosa</i> . Later the same species of cicada wing was found to kill only Gram-negative or less rigid bacterial cells. | 177, 231 |
| 2013 | dragonfly | <i>Diplacodes bipunctata</i> | nanopillars | diameter: 50–70 nm height: 240 nm | Tested against gram-negative <i>P. aeruginosa</i> cells, Gram-positive <i>Staphylococcus aureus</i> cells, and <i>Bacillus subtilis</i> spores. | 186 |
| 2015 | cicada | <i>Megapomponia intermedia</i> (ME) <i>Ayuthia spectabile</i> (AY) <i>Cryptotympana aguila</i> (CA) | nanopillars | height: 241 nm pitch: 165 ± 8 nm diameter: 156 ± 29 nm aspect ratio: 1.55 height: 182 nm pitch: 251 ± 31 nm diameter: 207 ± 62 nm aspect ratio: 0.88 height: 182 nm pitch: 187 ± 13 nm diameter: 159 ± 47 nm aspect ratio: 1.15 | Greater number of dead Gram-negative <i>Pseudomonas fluorescens</i> cells on ME and CA wings compared with AY wings. | 49 |
| 2016 | dragonfly | <i>Diplacodes bipunctata</i> (DI) <i>Hemianax papuensis</i> (HE) <i>Austroaeschna multipunctata</i> (AU) | nanopillars | height: 200–300 nm diameter: 80 ± 20 nm spacing: 180 ± 30 nm | Tested against Gram-negative <i>P. aeruginosa</i> cells, Gram-positive <i>B. subtilis</i> and <i>S. aureus</i> cells, and their spores. Killing efficiencies: HE < AU < DI | 181 |
| 2017 | damselfly | <i>Calopteryx hemorrhoidalis</i> | nanopillars | height: 433.4 ± 71.2 nm tip diameter: 47.7 ± 11.1 nm spacing: 116.1 ± 39.6 nm | Studied susceptibilities of <i>P. aeruginosa</i> and <i>S. aureus</i> at various stages of growth. | 180 |

amounts), were not killed by these nanopillars. Another study investigated the susceptibility of bacterial cells on the wing surfaces of *Calopteryx hemorrhoidalis* damselfly and the dependence on whether the bacteria are at their early logarithmic or stationary phase of physiological growth.¹⁸⁰ The microbes were more prone to mechanical rupturing during the early phases of growth compared with mature cells. Some comparative studies conducted among three different species of cicada wings⁴⁹ proved that the bactericidal effect is strongly affected by variations in the nanopillar dimensions (height, tip diameter, and spacing between pillars) from one species to another (Table 1). Interestingly, among the three species of dragonflies, which inhabit similar environments, the bactericidal efficacy imparted by the nanotopography of protrusions on their wings varied considerably.¹⁸¹ Two main lipid components of the insect wings, palmitic (C16) and stearic (C18) acids, have been crystallized to generate three-dimensional (3D) structures, which have been reported to exhibit bactericidal activity.¹⁸²

The bactericidal insect wings represent an excellent template for the development of synthetic antibacterial surfaces. The aim has been to design surfaces that can inhibit the attachment of microbes and effectively halt biofilm formation; this in turn prevents any subsequent infection of the surrounding tissue.^{175,183–185} The first physical bactericidal activity of a hydrophilic, synthetic surface of black silicon (bSi) was

reported recently.¹⁸⁶ For this work, high-aspect-ratio nanopillars inspired by the wings of the dragonfly *Diplacodes bipunctata* were generated and proved to be lethal for Gram-positive as well as Gram-negative bacteria (Figure 5). The biocompatibility of bSi was further investigated and demonstrated by in vivo implant studies. No inflammatory responses were found from the host in animal trials for both ocular and general tissue environments, suggesting possible biomedical applications.¹⁸⁴ Several other reports with the aim of engineering wing-inspired biomaterials have been published (Figure 5).^{185,187–190} However, wing-inspired strategies are not limited to implant surfaces but also have many other potential applications such as reducing nosocomial infections.^{190,191} Recently, Wang et al. incorporated dragonfly-inspired bSi into a reusable cell, resulting in a bactericidal microfluidic device.¹⁹² The device was shown to effectively rupture *Escherichia coli* cells from contaminated water. With adequate scalability, this could represent a viable method of cleaning bacteria-infected water sources without the need for cleansing chemicals. Generic or selective protection from microbial colonization could be conferred to surfaces for a wide spectrum of applications such as internal medicine, implants, food preparation, and agriculture by patterning the material surfaces or depositing coatings inspired by cicada and dragonfly wings. Recently, TiO₂ nanowires were generated using a simple hydrothermal treatment and were found to

mimic the killing behavior of insect wings.^{187,193} The discovery of bactericidal properties of insect wings has motivated research in diverse fields.^{54,194–196}

The antibacterial behavior of insect wings is closely related to their nanoscale topography and hydrophobicity. It has been observed that bactericidal wings are highly hydrophobic or superhydrophobic and have higher roughness or a unique nanoscale topography, all of which may be interrelated. However, the bactericidal activity is species-specific and varies according to the surface topography; this could be an evolutionary or behavioral change. For example, dragonflies have two dominant behaviors: perching and hawking. Perchers remain close to plants, where they wait for prey, while hawkers are in continuous flight hunting for prey. Percher dragonflies would need a wing that can fight microbes because its surrounding environment is more prone to microbial attacks. In contrast, the hawker can survive without such a surface property, as it spends more time in flight. In fact, it has recently been observed that the wings of perchers exhibit a surface topography that can kill microbes, whereas those of hawkers cannot kill microbes efficiently.¹⁸¹

■ BIOMIMICRY

Modeling and Simulation. Efforts to model the unique properties of insect wings have been focused primarily in two areas: (a) aerodynamic modeling, aiming to realize a special class of unmanned aerial vehicles (UAVs) called flapping-wing micro air vehicles (FWMAVs), and to a lesser extent (b) anti-biofouling surfaces, in which the goal is to elucidate the mechanism of biological interaction. MAVs, a miniature class of UAVs, have been the subject of extensive investigation in recent decades with potential uses in hazardous environments and for remote observations or surveillance. However, the aerodynamic principles governing flight at such small scales are remarkably different from those used in aircraft;¹⁹⁷ this has prompted research on insect and bird flight, where the flapping wing motion seems to be a concurrent solution.⁷¹ Engineers have attempted to build several prototypes of FWMAVs in the past two decades, few of which have achieved successful flight.¹⁹⁸ Calculation of aerodynamic forces and instantaneous modulation of wing kinematics are crucial in such prototypes since they will ensure control over the orientation of thrust and allow maneuverability and stability. Thus, an aerodynamic model that is capable of accommodating all of the high-lift unsteady aerodynamic effects exhibited by true insects is indispensable. A dynamic model also allows parameter variations to be tested in simulations before committing to building a new prototype, thereby saving both time and resources.

Pertaining to the low Reynolds number (10^2 – 10^3) fluid flow in aerodynamic situations, most models utilize the quasi-steady approximation as a foundation to develop the aerodynamic theory of insect flight.^{199,200} First, an averaged model is constructed assuming that fluid dynamic forces do not depend on their time history but depend only on instantaneous wing kinematics such as velocities and accelerations. This quasi-steady simplification allows changes in the angle of attack over time and velocity variation along the wingspan to be taken into consideration, unlike steady-state models; it also simplifies effects such as added mass, absence of stall, and rotational circulation into practicable equations.^{69,71,201–203} Mechanisms such as wake capture, Wagner effect, and clap and fling are excluded from almost all models because of poor under-

standing, although there have been attempts to include the last of these in quasi-steady models.²⁰⁴ Some models that incorporate rotational, translational, added mass, and viscous forces encountered during flight have been proposed.^{203,205} Many models treat the insect body and wings as several connected rigid bodies, in which the bodies representing the wings are associated with certain degrees of freedom (DoF). This allows determination of wing velocities and subsequently the forces and even torques generated by them.²⁰⁶ While the inclusion of greater DoF would permit greater accuracy and robustness in a model, it would also introduce new parameters, leading to greater mathematical complexity. Also, although the rigid-wing assumption is useful for understanding the essential flapping-wing aerodynamics, the insect wings undergo 3D elastic deformation in terms of chordwise, spanwise, and twist deformation during flapping flight.²⁰⁷ The aerodynamics and structural dynamics of insect wings result in complex fluid–structure interaction (FSI) phenomena that enhance the aerodynamic power generated, which must be accommodated into models for greater accuracy.^{208,209}

The computational fluid dynamics (CFD) method is capable of computing aerodynamic forces and detailed flow structures by directly solving the Navier–Stokes equations by numerical methods.²¹⁰ However, this approach sacrifices simplicity and hence the applicability of quasi-steady models in FWMAVs. Similar to quasi-steady models, CFD primarily involves defining simplified model geometries based upon direct measurements of animals. A kinematic model is then prescribed, replicating the observed parameters at different time points during a stroke, and the wing models are encapsulated in overset meshes. The computational background is meshed with refined grids near the wings that become larger and sparser further away from the wing surface. The Navier–Stokes equation can then be applied to calculate aerodynamic parameters. The studies can generate either 2D²¹¹ or 3D models; the latter are more complicated and have gained prominence among researchers only recently, after it was demonstrated that 2D models may be inadequate for capturing 3D effects such as spanwise flow in larger insects.^{212,213}

FWMAVs often use rotary electric motors as a means of propulsion for actuators, and therefore, the rotary motion needs to be efficiently translated to flapping motion. A recent study demonstrated that the Scotch yoke mechanism for actuators mimics the wing-tip motions of *Manduca sexta* better than other mechanisms, making it a viable option for application in a robotic moth.²¹⁴ Bioinspired flight simulators for generating and collecting data rather than constructing MAVs or taking direct measurements from captured insects may help to avoid the tough experimental challenge of large amounts of information capture for proper investigation of 3D near and far flow fields.^{197,215} Such simulators may be used to optimize the physical geometry and material properties of components by simulating internal forces and energy losses, thereby reducing the number of hardware iterations.

Each of the proposed models can address various aspects of insect flight with varying degrees of accuracy because certain features (e.g., wing and body aerodynamics) are encompassed in a model more easily than others (e.g., neural circuitry and wing hinge mechanics). Insects rely on the provision of rich sensory feedback from multiple sensors such as compound eyes, ocelli, and antennae, which endow them with inherent flight stability by allowing them to modulate parameters such

as beat frequency and angle of attack instantaneously. Thus, to achieve similar results in FWMAVs, the models need to be computationally robust and capable of modulating the power output and structural dynamics according to sensory inputs.⁶⁴ Moreover, there are notable differences in the flight dynamics of large and small insects and in two- and four-winged ones,²¹³ ranging from large differences in stroke amplitude or flapping frequency to altogether dissimilar flight mechanisms.⁸³ Therefore, formulating a unified model that applies to a broad range of insects seems to be a nontrivial task at this point.

In the case of modeling bactericidal insect wings, the bacterial membrane undergoes stretching once it is in contact with the nanoarchitecture. Therefore, there is a stretching free energy penalty and a decrease in free energy due to contact adhesion of the membrane to the surface. There also exists an energy penalty for the bending energy change, which some models choose to ignore since the curvature is negligible compared with the cell dimensions. In the current models, bacterial cell membranes are assumed to be thin elastic layers whose structural details and composition can then be neglected. This assumption is reasonable since the thickness of bacterial cell walls is an order of magnitude smaller than the dimensions of the nanostructures. However, complex models are needed that consider randomly oriented nanopillar geometries and a dynamic cell rather than a simple layer.

The phenomenological model proposed by Pogodin et al. is based on the concept that adsorption of bacteria onto surface nanopillars is due to the decrease in contact adhesion energy; this leads to stretching of bacterial cell walls suspended between the nanopillars, which causes an increase in the free energy.¹⁷⁹ An equilibrium is reached as these competing effects cancel each other. Their model correctly predicts that Gram-positive bacteria, possessing comparatively rigid and thick cell walls, are more difficult to deform than the more flexible walls of Gram-negative bacteria. This prediction was verified by decreasing the rigidity of surface-resistant strains through microwave irradiation of the cells, which rendered them susceptible to the bactericidal mechanisms of wing surfaces. Li proposed an analytic thermodynamic model, analyzing the total free energy change of bacterial cells adhered to the patterned surface.²¹⁶ This model considered all the three processes described above that contribute to a change in free energy. However, the shape of bacterial cells was taken to be spherical because of the difficulty in quantitatively calculating the relation between the geometrical shape parameters during adhesion of rod-shaped bacteria. Ye et al. developed a biophysical model similar to the model of Pogodin et al. that describes the change in total free energy of an adherent *Candida albicans* cell on nanofiber-coated surfaces as a function of the geometry and configuration of the surface topology.²¹⁷ Polystyrene (PS) nanofiber-coated substrata were fabricated, and experiments were conducted to quantify the cell attachment density for various fiber diameters at a prescribed spacing in support of their model. Other models that may be useful in further understanding the bacterial killing mechanism include the bead model or single-chain molecular theory, which is already used in the modeling of membrane phospholipid bilayers.²¹⁸

Fabrication Strategies. Bioinspiration involves emulating ideas from nature. A key challenge in this endeavor is the need for fabrication and manufacturing strategies, especially in the mimicking of insect wings. As insect wings possess a variety of unique properties, the fabrication technique must depend on

the targeted property. Once the intended property has been identified and a possible route of fabrication has been designed, currently available techniques may be utilized, or the development of new tools may be required. The fabrication of insect-wing-inspired structures has been on the rise since micro- and nanoreplication strategies have become prevalent in the past decade (Table 2). Earlier, simple ornithopters such as MAVs were made to study aerodynamic properties and, more recently, to study sensing applications.^{219–221} However, to accurately mimic insect wing properties, advanced fabrication methods such as the micromolding technique, also known as soft lithography, must be used. Here, plastic is pressed on a master mold (or stamp) to replicate patterns. Micromolding can easily transfer the wing and its corrugated structures.^{222,223} If the right plastic (i.e., with the desired characteristics) is chosen, then this technique can transfer microscale defects and features. Other similar techniques such as photolithography, electron beam lithography, hot embossing, and nanoimprint lithography have been used in mimicking insect wings.^{153,224–227} The primary difference lies in using either heat, light, or electrons as the source while transferring the features from the mold to the plastic. In some cases, the mold is designed through computer software and then fabricated using a laser, whereas in others insect wings are directly used as a mold.²²⁴ In biotemplating, the wing is used as a mold.^{146,147,154,227,228}

In most lithography techniques, the transfer of patterns is completed by a final etching step that is performed by reactive ion etching (RIE) or wet etching techniques. Recently the nanoscale features of dragonfly wings that are more random than patterned were fabricated using a one-step etching technique^{186,188,229} in which a few processing parameters can be optimized to generate the random roughness. RIE and lithography have limited scalability, in contrast to random wet etching, which is relatively more scalable.²²⁹ Similar to wet etching, hydrothermal treatment has also been employed to generate nanopillars on titanium.^{187,193} Although this treatment involves a greater number of steps and extremely high process temperatures, there is more control of the geometry compared with random wet etching. The anodization of aluminum is another significant electrochemistry-based process that is also scalable to generate nanopillars.²³⁰ In the first step, electrochemical oxidation occurs, and an ordered anodic aluminum oxide (AAO) is formed. In the second step, reduction takes place on the surface, such as deposition of metals or galvanic deposition.

Another technique is focused ion beam (FIB) milling, in which a focused beam of ions such as gallium can be used to mill or excavate the materials to generate desired geometries.¹⁹⁵ Although FIB milling has never been employed to mimic an insect wing, probably because it is slow and expensive, it can be a good technique to characterize the cross sections of insect wing nanofeatures.²³¹ Sol-gel is a synthetic approach based on biotemplates to make metal oxide nanofeatures.¹⁴⁶ Metal oxides such as TiO₂ are rapidly formed in steps of hydrolysis, condensation, and drying. This is a low-cost method, like most wet chemical techniques. The precision, robustness, cost, and ability to replicate complex 3D structures of current fabrication methods are limited.²⁵²

The fabricated materials can be single-layered (consisting of grooves, pillars, or other architectures on a single sheet^{154,228}), multilayered (prepared by stacking or deposition of layers^{132,233}), or quasi-ordered. Often the designed process is

Table 2. Different Kinds of Insect-Wing-Based Bioinspiration To Achieve Multifunctional Materials^{4a}

| year | insect | bioinspiration | material; nanotopology | geometry | fabrication method | remarks | ref |
|------|---|---------------------|---|--|---|--|-----|
| 2004 | <i>Morpho</i> butterfly | optics | quartz patterned substrate, with TiO ₂ and SiO ₂ layers on top; multilayered quasi-ordered structures | layer thicknesses: TiO ₂ , ~40 nm; SiO ₂ , ~75 nm; 14 layers total substrate unit: 300 × (2000 ± SD) nm ² | electron beam lithography and dry etching for patterning the substrate; electron beam deposition for layers | two-step fabrication capable of emulating almost all aspects of <i>Morpho</i> wings | 237 |
| 2005 | <i>Morpho</i> butterfly | optics | diamondlike carbon; treelike nanostructures | height: 2.6 μm length: 20 μm width: 0.26 μm grating pitch: 0.23 mm | focused ion beam milling, chemical vapor deposition (CVD) | nearly the same shape and size as <i>Morpho</i> scales; process is expensive and slow | 238 |
| 2006 | <i>Morpho</i> butterfly | optics | UV curable resin for patterned substrate, TiO ₂ and SiO ₂ layers on top; multilayered quasi-ordered structures | layer thicknesses: TiO ₂ , ~40 nm; SiO ₂ , ~75 nm; 14 layers total substrate unit: 300 × (2000 ± SD) nm ² | nanocasting lithography on the substrate; electron beam deposition for layers | low-cost, scalable reproduction method for <i>Morpho</i> butterflies; can be used for other colors too | 163 |
| 2006 | <i>Morpho peleides</i> butterfly | optics | Al ₂ O ₃ ; inverted structure of the original | 10, 20, 30, and 40 nm thick layers deposited on template | biotemplating using low-temperature atomic layer deposition (ALD) | tunable color depending on layer thickness; successfully replicated morphological and optical properties of the wing | 139 |
| 2007 | <i>Morpho sulkowskyi</i> butterfly | optics, sensors | Christmas-tree-like nanostructures without modification | — | — | demonstrated vapor selectivity and sensitivity of butterfly scales for the first time | 150 |
| 2008 | <i>Battus philenor</i> butterfly | optics | chalcogenide glass | layer thickness: 0.5 μm | biotemplating using conformal evaporated film by rotation | replicated optical characteristics of the wing | 239 |
| 2008 | <i>Cryptohypnana atrata</i> Fabricius cicada | optics | PMMA polymer films; conical nanopillars | height: 440 nm spacing: 185 nm diameter: 140 nm (base), 55 nm (top) | replica molding | photonic structure with antireflective property | 168 |
| 2009 | cicada | wettability | PTFE film for membrane, carbon/epoxy fibers for veins | PTFE film: 150 μm nanostructures on film: height, 200 nm; width, 1.2 μm "veins": carbon/epoxy, 100 μm wing mass: 1.9 g wingspan: 17.5 cm | argon and oxygen ion beam treatment for nanostructures, thermal treatment | superhydrophobic, low-cost, flexible process, but inertial characteristics such as bending etc. were not evaluated | 127 |
| 2009 | <i>Cylichila australasiae</i> cicada | sensors | h-PDMS; nanopillars | spacing: 50 nm diameter: 110 nm height: 200 nm | nanoimprint lithography | integrated a nanoscale biological template with optical fiber to produce highly sensitive SERS probes | 170 |
| 2010 | <i>Papilio blumei</i> butterfly | optics | Pt or Au substrate having an array of concavities; alternating layers of Al ₂ O ₃ and TiO ₂ deposited on top | concavities: diameter, 4.5 μm; height, 2.3 μm layer thicknesses: Al ₂ O ₃ , 82 ± 4 nm; TiO ₂ , 57 ± 4 nm | colloidal self-assembly, sputtering, ALD | adjusting the fabrication parameters also allows mimicking of either the single color of <i>Papilio ulyses</i> or the color mixing of <i>Papilio palinurus</i> | 132 |
| 2011 | <i>Morpho menelaus</i> butterfly | wettability, optics | Al ₂ O ₃ ; naturally occurring "Christmas tree" structures | ridge height: 1.8 μm spacing: 0.8 μm | biotemplating using low-temperature ALD | high-aspect-ratio nanostructures; homologous iridescence and diffraction | 161 |
| 2011 | <i>Papilio palinurus</i> butterfly | optics | Al ₂ O ₃ and TiO ₂ layers on a PS film with concavities | concavities: 4–5 μm five alternating layers of 20 nm thickness | breath-figure-templated assembly, ALD | emulated double reflection, polarization, and polarization effects exhibited by the insect | 240 |

Table 2. continued

| year | insect | bioinspiration | material; nanotopology | geometry | fabrication method | remarks | ref |
|------|---|-------------------------------------|--|--|---|---|-----|
| 2011 | <i>Euploea mulciber</i> butterfly | optics, micro- and nanoarchitecture | Co, Ni, Cu, Pa, Ag, Pt, and Au; metal layers deposited on naturally occurring nanoscale ridges, struts, and ribs | layer thicknesses: ridges and struts, 20–50 nm; ribs, 20–30 nm | selective surface functionalization, electroless deposition | versatile method capable of replicating a wide range of metallic substrates | 232 |
| 2011 | <i>Nephotoma appendiculata</i> crane fly | aerodynamics | SU-8 for veins, PDMS for membrane | varying width and thickness of “veins” and membrane span of one wing: 7.5–20 μm | advanced microelectromechanical systems (MEMS) technology | slow and expensive fabrication process; although it faithfully mimicked material conception, weight, venation, size, mass distribution, and wing rigidity, the wing mass was considerably larger than those of natural counterparts | 241 |
| 2012 | <i>Morpho</i> butterflies | optics, micro- and nanoarchitecture | alternating layers of SiO ₂ and Si ₃ N ₄ on Si substrate; treelike nanostructures | ridge width: 250 nm lamella width: 50 nm period: 500 nm | CVD, UV lithography, reactive ion etching (RIE), wet etching | possible to mimic the complexity of most species of butterfly wings using a combination of isotropic and anisotropic RIE | 234 |
| 2012 | <i>Morpho</i> butterflies | sensors | wing scales doped with SWCNTs | lamella spacing: 150 nm ridge spacing: 770 nm | surface functionalization | midwave IR detection with high sensitivity and response speed | 242 |
| 2013 | <i>Diplacodes bipunctata</i> dragonfly | antibacterial activity | silicon; nanopillars | diameter: 20–80 nm height: 500 nm | RIE | first reported physical bactericidal activity of any surface | 186 |
| 2013 | <i>Papilio blumei</i> butterfly | optics | Si substrate with an array of concavities, with alternating layers of Ta ₂ O ₅ and SiO ₂ on top | concavity radii: 4 μm layer thickness different for each layer | self-assembly, electron-beam deposition, and inductively coupled plasma etching | multilayered stacks, no use of biotemplate | 233 |
| 2013 | <i>Morpho sulkowskyi</i> butterfly | optics | PMMA; several treelike structures with different dimensions of the ridges | structures lie flat on the substrate, height \approx 150 nm | electron-beam lithography | investigation of how the structure geometry affects optical phenomena exhibited by the insect | 243 |
| 2013 | <i>Morpho sulkowskyi</i> butterfly | sensors | honeycomb-shaped network of SWCNTs self-assembled on wing scales | – | biotemplating; self-assembly | demonstrated laser-triggered remote heating, high electrical conductivity, and repetitive DNA amplification | 244 |
| 2014 | cicada | antibacterial activity | titanium; nanowires | fine: 100 nm diameter coarse: 10–15 μm diameter | alkaline hydrothermal process | selectively bactericidal while supporting cell proliferation patterns, which is dependent on array geometry | 187 |
| 2014 | <i>Morpho</i> butterfly | optics | SiO ₂ and TiO ₂ on Si; nanopillars | height: 3 μm layer thicknesses: SiO ₂ , 73 nm; TiO ₂ , 38 nm | spin coating, dry etching, Cr deposition, SiO ₂ /TiO ₂ deposition | investigation of the effect of nanoscale disorder in <i>Morpho</i> -inspired surfaces | 245 |
| 2014 | <i>Pierella luna</i> butterfly | optics | UV-curable epoxy resin; microplate array | plate: length, 10 μm ; height, 8 μm ; width, 2 μm | replica molding | fabricated a photonic system with periodic arrangements of diffraction elements; nonexistent in its natural inspiration | 141 |
| 2015 | <i>Papilio blumei</i> , <i>Cicindela chinensis</i> , <i>Papilio peranthus</i> , and <i>Sunew coronata</i> butterflies | optics | cylindrical and triangular grooves with layers of TiO ₂ and Al ₂ O ₃ | spacing: perpendicular, 12 μm ; collinear, 15 μm nine alternating layers; depth of grooves not characterized | photolithography, RIE, plasma-enhanced ALD | grooves exhibit angle dependence of the polarization and color | 246 |
| 2015 | cicada | optics | PET; nanopillars | different etch times produce pillars with different dimensions | colloidal self-assembly, RIE, wet etching | investigation of how the ARS performance depends on fabrication parameters such as the etch time | 247 |
| 2015 | <i>Morpho</i> butterfly | optics, sensors | PMMA treelike nanostructures functionalized with fluorine-terminated silane or 3-aminopropyltrimethoxysilane | lamella thickness: 86 \pm 6 nm | electron-beam lithography, vapor deposition | capable of quantifying vapors in mixtures and when blended with a variable-moisture background | 148 |

Table 2. continued

| year | insect | bioinspiration | material; nanotopology | geometry | fabrication method | remarks | ref |
|------|---|-------------------------------------|--|---|---|--|-----|
| 2015 | cicada | optics | Si and Ge; hexagonal nanotip arrays | different arrays with different dimensions | plasma etching | nanotip arrays for efficient light harvesting over a 300–1000 nm spectrum and up to a 60° angle of incidence in both low- and high-index materials | 248 |
| 2015 | dragonfly | antibacterial activity, wettability | silicon; nanopillars | height: 4 μm diameter: 220 nm random interpillar spacing | deep RIE | "super" surface killed Gram-positive (<i>S. aureus</i>), Gram-negative (<i>E. coli</i>), and mammalian (mouse osteoblast) cells with high efficiency | 188 |
| 2016 | <i>Trigonoptera brookiana</i> butterfly | optics | SiO ₂ nanoditch array | cover scales: ridge width, 383 nm; spacing, 990 nm ground scales: ridge width, 508 nm; spacing, 2.08 μm | sol-gel, selective wet etching | simple biotemplating method for preparing small-scale replicas | 133 |
| 2016 | <i>Dione juno</i> butterfly | optics | fused SiO ₂ substrate and IP-L 780 photoresist; zigzag shapes | thickness: 0.3 μm height: 1.6 μm various periodicities | direct laser writing | demonstrated substrate-independent resonance, upscaling using controlled buckling is possible | 156 |
| 2016 | cicada | optics, wettability | PDMs; nanopillars | diameter: 150 nm (top), 250 nm (bottom) pitch: 720 nm height: 200–300 nm | biotemplating by replica molding | antireflective and superhydrophobic characteristics were inherited | 249 |
| 2016 | <i>Cryptotympana atrata</i> Fabricius cicada | optics | biomorphic TiO ₂ nanopillars | height: 230 ± 42 nm spacing: 250 ± 18 nm diameter: 75 ± 4 nm (top), 175 ± 10 nm (basal) | sol-gel process | demonstrated angle-dependent antireflectivity | 146 |
| 2016 | <i>Callophrys rubi</i> butterfly | optics | organic photoresin; 3D gyroid | 20 μm × 20 μm × 4 μm samples | optical two-beam super-resolution lithography | controllable structural handedness and possible complete band gap | 250 |
| 2016 | dragonfly | antibacterial activity | black silicon; nanopillars | height: 652 ± 10.3 nm tip diameter: 100 ± 1.8 nm density: 12.2 pillars/μm ² | RIE | In vivo studies demonstrated biocompatibility, reduced inflammation, and bactericidal nature | 184 |
| 2016 | dragonfly | antibacterial activity | black silicon; nanopillars | height: 500 nm diameter: 95 nm | RIE | fabricated a reusable bactericidal microfluidic device with several potential applications | 192 |
| 2017 | cicada and dragonfly | antibacterial activity | titanium; nanofibers | spacing: 450 ± 200 nm fine: diameter, 34 ± 6.5 nm; tip-to-tip spacing, 171.3 ± 48.3 nm coarse: diameter, 7.78 ± 2.56 nm | hydrothermal treatment | integrated topological and biochemical cues (ligands) to achieve a bactericidal surface that also supports osseointegration | 251 |
| 2017 | <i>Morpho didius</i> butterfly | optics | SiO ₂ , SiN _x ; multilayered conical treelike structures | approximate ledge height: 30 nm | CVD, metal nanoparticle formation, wet-chemical etching | high transmission of infrared light and strong reflection of visible light at high angle | 157 |
| 2017 | <i>Cryptotympana atrata</i> Fabricius cicada | optics, wettability | biomorphic SiO ₂ ; conical nanopillars | height: 190 ± 25 nm tip spacing: 290 ± 28 nm tip diameter: 63 ± 3 nm basal diameter: 260 ± 33 nm | biotemplating by ultrasonic assisted sol-gel method | angle-dependent antireflection and enhanced hydrophilic properties | 147 |

Table 2. continued

| year | insect | bioinspiration | material; nanotopology | geometry | fabrication method | remarks | ref |
|------|--|---|---|--|---|--|-----|
| 2017 | <i>Cryptohympana atrata</i> Fabricatus cicada | optics, wettability, micro- and nanoarchitecture | polystyrene; tapered nanopillars | height: 156 nm spacing: 180 nm | electroless plating, electroplating, microinjection compression molding | hydrophobic and antireflective replica prepared by biotemplating | 169 |
| 2018 | dragonfly | antibacterial activity, micro- and nanoarchitecture | black silicon; nanopillars | multiple samples with varying pillar height and density | RIE | investigation to correlate topographical characteristics to bactericidal efficiency | 189 |
| 2018 | generic | antibacterial activity | aluminum and its alloys; hierarchical structure of micro- and nanoscale pillars | roughness characterized using various roughness parameters such as R_{rms} , R_a , etc. | wet etching | resisted attachment of drug-resistant bacterial strains collected from hospital environments; highly scalable | 229 |
| 2018 | <i>Morpho sulkowskyi</i> butterfly | optics | ZnO; naturally occurring treelike nanostructures | layers of various thicknesses deposited on the wing nanostructures | low-temperature ALD ($T < 150\text{ }^\circ\text{C}$) | tunable color, providing aesthetic properties and simultaneously enhancing photocatalytic activity; demonstrated possible uses in water purification | 154 |
| 2018 | <i>Chorinea faunus</i> butterfly | optics, antibacterial activity, micro- and nanoarchitecture | Si_3N_4 ; disk-shaped nanostructures | disk shapes with various radii aspect ratio: 0.45 | phase-separation-based polymer assembly process | engineered biophotonic, anti-biofouling, nanostructured surface and demonstrated in vivo applicability | 104 |
| 2018 | <i>Morpho peleides</i> butterfly | optics, sensors | wing scales embedded into PVA | natural nanostructures | infiltrating scales with PVA | demonstrated pH sensitivity | 252 |

*Abbreviations: PMMA, poly(methyl methacrylate); PTFE, polytetrafluoroethylene; PET, poly(ethylene terephthalate); PDMS, polydimethylsiloxane; PVA, poly(vinyl alcohol).

a combination of techniques, such as that performed by Aryal et al. to mimic large-area complex 3D ultrastructures of a *Morpho* butterfly's wing scale; the process included chemical vapor deposition, photolithography, and chemical etching.²³⁴ Another combination strategy includes colloidal self-assembly, sputtering, and atomic layer deposition to fabricate multiple-layer structures inspired by butterfly wings.¹³² Recently, inspired by the wings of *Chorinea faunus* butterflies, Narasimhan et al. engineered a transparent photonic nanostructured silicon nitride (Si_3N_4) membrane exhibiting structurally induced scattering;¹⁰⁴ in vivo studies proved this membrane to be suitable for IOP-sensing implants. Some methods to maximize the amount of light energy captured have been devised, inspired from angle-dependent reflection.^{146,147} These studies highlight the untapped potential of biomimetic surfaces and their likely impact in the near future.

To mimic complete insect wings, fabrication must start at the bottom. Initially, nanoscale or even smaller features need to be fabricated. The corrugations and complex vein systems can be generated using molding techniques. Mimicking of insect wings is heavily dependent on physics or rather the growth of nanofabrication tools and processes. Application-dependent techniques can be employed to further characterize and study the fascinating properties of insect wings, and a combination of these techniques can possibly offer novel insights.

CONCLUSIONS AND FUTURE PERSPECTIVES

Despite centuries of investigations on insects, many wing characteristics have not yet been discovered or understood. To start, there is a lack of search engines or databases on categorization of insect wings. DrawWing is one of the wing-image analysis softwares that has been utilized for identification of insects by giving a numerical description of the wings. A robust digitization is required, which can be accomplished by collaborative efforts between entomologists and computer scientists.

The mechanical, biological, mechanoresponsive, optical, and aerodynamic properties are not fully understood. Although aerodynamics has been the most researched area with respect to insect wings, there is still scope to investigate the effect of different wing shapes and wing-surface structures on flight kinetics. The optical properties remain another extensive research topic that has inspired scientists to fabricate wing-inspired photonic materials. The surface characteristics such as wettability, anisotropy, reflectance, and self-cleaning have been researched by dedicated groups who have characterized the wings of different species but of the same order. The wings across insect orders can be characterized. There is a need to relate the wing surface with its many functions. A future approach would be to find a mathematical relationship between surface features and different properties or a structure–multifunction relationship; also, the interdependence of properties should be studied.

One of the promising fields is the interaction of biological organisms on the surface of insect wings, which was highlighted with the discovery of bacteria-killing cicada wings. Since 2012, efforts to understand and mimic the bactericidal behavior of insect wings have increased rapidly. With the growing concern over multidrug-resistant bacteria and hospital-acquired infections, killing through physical contact offers a novel alternative approach to possibly minimize the spread of such infections. Because of the presence of micro- and nanoscale patterns on insect wings,

modeling of their geometries is possible, and their interaction with cells can be understood in detail. The fabrication of wing-inspired nanoscale patterns is still in its infancy, probably because generally the fabrication tools for nanoscale pillars on surfaces are expensive and technically challenging. For the generation of patterns, a clean-room environment and state-of-the-art fabrication technologies are required. These techniques are expensive, and wing-inspired surfaces cannot be produced at high throughput. In the field of nanotechnology, almost all progress has been made in the area of nanoparticles that are synthesized in solution. Very few techniques offer the synthesis of stable and standing nanopillars or nanofeatures on solid substrates similar to the nanoarchitectures found on insect wings. Therefore, there is a need to extensively focus on the fabrication of stable geometries at the nanoscale, inspired by insect wing surface topography.

It is also important to consider the application before designing insect-wing-inspired surfaces. If the surfaces are designed to resist bacterial infections for biomedical implants, then many other factors play complex roles. There is a race of eukaryotic cells against bacterial cells, which should be given due importance during the design of nanopillars. Rapid initiation of a biological cascade occurs at the surface as a result of monocyte and macrophage adhesion, coagulation, protein adsorption, remodeling, inflammation, and deposition of extracellular matrix.^{235,236} Therefore, it is plausible that the nanopillars are ineffective against bacterial cells in vivo. However, the same nanopillar surface may show efficient bacterial killing in vitro. In the case of insect wings, they can easily kill bacterial cells because of the different surrounding habitats and environmental conditions. Although wing nanopillars demonstrate antibacterial activity, mimicking the exact topography may not be a smart design for implants. A better strategy would be to optimize the surface topography in addition to other currently used modifications or coatings when considering bioinspiration in the field of medical devices. However, the design of the topography of insect wings may benefit other industries such as food processing.

In conclusion, insect wings continue to fascinate and inspire researchers in various fields with their hitherto-unknown properties and several unexplored opportunities that need investigation. There is enormous scope for developing a better understanding of the mechanisms underlying the known properties and finally engineering strategies to replicate them synthetically to address societal needs.

■ ASSOCIATED CONTENT

📄 Supporting Information

The Supporting Information is available free of charge on the ACS Publications website at DOI: [10.1021/acsbomaterials.9b00217](https://doi.org/10.1021/acsbomaterials.9b00217).

A table listing the discovery of micro- and nanoscale architecture and wettability of insect wings and a figure illustrating the citation analysis of publications of insect wings in specific areas (PDF)

■ AUTHOR INFORMATION

Corresponding Authors

*E-mail: kchatterjee@iisc.ac.in.

*E-mail: y.prasad@qut.edu.au.

ORCID

Kaushik Chatterjee: 0000-0002-7204-2926

Prasad K. D. V. Yarlagadda: 0000-0002-7026-4795

Notes

The authors declare no competing financial interest.

■ ACKNOWLEDGMENTS

The authors are grateful to Mr. Rikuto Kuraishi, Mr. Enguerrand Masse Apere, and Mr. Lars Kristensen for providing high-resolution photographs of insects and thank Ms. Rinsha Padmarajan for assistance with the literature search. P.K.D.V.Y. acknowledges funding from the VAJRA Program of the Science and Engineering Research Board (SERB), Department of Science & Technology (DST), Government of India (GOI). The funding from the Department of Biotechnology (DBT), GOI, for the Bioengineering and Bodesign Initiative – Phase 2 is gratefully acknowledged.

■ REFERENCES

- (1) Nicholson, D. B.; Ross, A. J.; Mayhew, P. J. Fossil evidence for key innovations in the evolution of insect diversity. *Proc. R. Soc. B* **2014**, *281* (1793), 20141823.
- (2) Rees, C. J. C. Form and function in corrugated insect wings. *Nature* **1975**, *256*, 200.
- (3) Chabrier, J. *Essai sur le vol des insectes*; A. Belin: Paris, 1823.
- (4) Kirby, W.; Spence, W. *An Introduction to Entomology, or Elements of the Natural History of Insects*; Longman, Rees, Orme, Brown, and Green, 1828; Vol. 1.
- (5) Clark-Hachtel, C. M.; Tomoyasu, Y. Exploring the origin of insect wings from an evo-devo perspective. *Curr. Opin. Insect Sci.* **2016**, *13*, 77–85.
- (6) Alexander, D. E. A century and a half of research on the evolution of insect flight. *Arthropod Struct. Dev.* **2018**, *47* (4), 322–327.
- (7) Hamilton, K. G. A. The insect wing, Part I. Origin and development of wings from notal lobes. *J. Kansas Entomol. Soc.* **1971**, *44* (4), 421–433.
- (8) Rasnitsyn, A. P. A modified paranotal theory of insect wing origin. *J. Morphol.* **1981**, *168* (3), 331–338.
- (9) Kukalova-Peck, J. Origin and evolution of insect wings and their relation to metamorphosis, as documented by the fossil record. *J. Morphol.* **1978**, *156* (1), 53–125.
- (10) Kukalova-Peck, J. Origin of the insect wing and wing articulation from the arthropodan leg. *Can. J. Zool.* **1983**, *61* (7), 1618–1669.
- (11) Gegenbaur, C. *Grundzüge der vergleichenden Anatomie*; W. Engelmann, 1870.
- (12) Müller, F. Beiträge zur Kenntniss der Termiten. IV. Die Larven von *Calotermes rugosus* Hag. *Jena. Z. Naturwiss.* **1875**, *IX*, 241–264.
- (13) Averof, M.; Cohen, S. M. Evolutionary origin of insect wings from ancestral gills. *Nature* **1997**, *385*, 627.
- (14) Niwa, N.; Akimoto-Kato, A.; Niimi, T.; Tojo, K.; Machida, R.; Hayashi, S. Evolutionary origin of the insect wing via integration of two developmental modules. *Evol. Dev.* **2010**, *12* (2), 168–176.
- (15) Dudley, R.; Pass, G. Wings and powered flight: Core novelties in insect evolution. *Arthropod Struct. Dev.* **2018**, *47* (4), 319–321.
- (16) Linz, D. M.; Tomoyasu, Y. Dual evolutionary origin of insect wings supported by an investigation of the abdominal wing serial homologs in *Tribolium*. *Proc. Natl. Acad. Sci. U. S. A.* **2018**, *115* (4), E658–E667.
- (17) Prokop, J.; Pecharová, M.; Nel, A.; Hörschemeyer, T.; Krzemińska, E.; Krzemiński, W.; Engel, M. S. Paleozoic nymphal wing pads support dual model of insect wing origins. *Curr. Biol.* **2017**, *27* (2), 263–269.
- (18) Grimaldi, D.; Engel, M. S. *Evolution of the Insects*; Cambridge University Press: Cambridge, U.K., 2005.
- (19) Stork, N. E.; McBroom, J.; Gely, C.; Hamilton, A. J. New approaches narrow global species estimates for beetles, insects, and

terrestrial arthropods. *Proc. Natl. Acad. Sci. U. S. A.* **2015**, *112* (24), 7519–7523.

(20) Truman, J. W.; Riddiford, L. M. The origins of insect metamorphosis. *Nature* **1999**, *401*, 447.

(21) Gullan, P. J.; Cranston, P. S. *Insects: An Outline of Entomology*; Wiley: Hoboken, NJ, 2004.

(22) Comstock, J. H.; Needham, J. G. The Wings of Insects. Chapter II. The Venation of Atypical Insect Wing. *Am. Nat.* **1898**, *32* (374), 81–89.

(23) Hamilton, K. G. A. The Insect Wing, Part II. Vein Homology and the Archetypal Insect Wing. *J. Kansas Entomol. Soc.* **1972**, *45* (1), 54–58.

(24) Wootton, R. J. Function, homology and terminology in insect wings. *Syst. Entomol.* **1979**, *4* (1), 81–93.

(25) Comstock, J. H.; Needham, J. G. The Wings of Insects. Chapter III. The Specialization of Wings by Reduction. *Am. Nat.* **1898**, *32* (376), 231–257.

(26) Hamilton, K. G. A. The Insect Wing, Part III. Venation of the Orders. *J. Kansas Entomol. Soc.* **1972**, *45* (2), 145–162.

(27) Hopkins, T. L.; Kramer, K. J. Insect cuticle sclerotization. *Annu. Rev. Entomol.* **1992**, *37* (1), 273–302.

(28) Vincent, J. F. V.; Wegst, U. G. K. Design and mechanical properties of insect cuticle. *Arthropod Struct. Dev.* **2004**, *33* (3), 187–199.

(29) Hadley, N. F. The Arthropod Cuticle. *Sci. Am.* **1986**, *255* (1), 104–113.

(30) Ivanova, E. P.; Nguyen, S. H.; Webb, H. K.; Hasan, J.; Truong, V. K.; Lamb, R. N.; Duan, X.; Tobin, M. J.; Mahon, P. J.; Crawford, R. J. Molecular Organization of the Nanoscale Surface Structures of the Dragonfly *Hemianax papuensis* Wing Epicuticle. *PLoS One* **2013**, *8* (7), No. e67893.

(31) Nguyen, S. H. T.; Webb, H. K.; Hasan, J.; Tobin, M. J.; Crawford, R. J.; Ivanova, E. P. Dual role of outer epicuticular lipids in determining the wettability of dragonfly wings. *Colloids Surf., B* **2013**, *106*, 126–134.

(32) Andersen, S. O. Biochemistry of insect cuticle. *Annu. Rev. Entomol.* **1979**, *24* (1), 29–59.

(33) Appel, E.; Heepe, L.; Lin, C. P.; Gorb, S. N. Ultrastructure of dragonfly wing veins: composite structure of fibrous material supplemented by resilin. *J. Anat.* **2015**, *227* (4), 561–582.

(34) Michels, J.; Gorb, S. Detailed three-dimensional visualization of resilin in the exoskeleton of arthropods using confocal laser scanning microscopy. *J. Microsc.* **2012**, *245* (1), 1–16.

(35) Haas, F.; Gorb, S.; Blickhan, R. The function of resilin in beetle wings. *Proc. R. Soc. London, Ser. B* **2000**, *267* (1451), 1375–1381.

(36) Gorb, S. N. Serial elastic elements in the damselfly wing: mobile vein joints contain resilin. *Naturwissenschaften* **1999**, *86* (11), 552–555.

(37) Donoughe, S.; Crall, J. D.; Merz, R. A.; Combes, S. A. Resilin in dragonfly and damselfly wings and its implications for wing flexibility. *J. Morphol.* **2011**, *272* (12), 1409–1421.

(38) Haas, F.; Gorb, S.; Wootton, R. Elastic joints in dermapteran hind wings: materials and wing folding. *Arthropod Struct. Dev.* **2000**, *29* (2), 137–146.

(39) Nijhout, H. F.; Callier, V. Developmental Mechanisms of Body Size and Wing-Body Scaling in Insects. *Annu. Rev. Entomol.* **2015**, *60* (1), 141–156.

(40) Johansson, F.; Söderquist, M.; Bokma, F. Insect wing shape evolution: independent effects of migratory and mate guarding flight on dragonfly wings. *Biol. J. Linn. Soc.* **2009**, *97* (2), 362–372.

(41) Parchem, R. J.; Perry, M. W.; Patel, N. H. Patterns on the insect wing. *Curr. Opin. Genet. Dev.* **2007**, *17* (4), 300–308.

(42) Stühr, S.; Truong, V. K.; Vongsvivut, J.; Senkbeil, T.; Yang, Y.; Al Kobaisi, M.; Baulin, V. A.; Werner, M.; Rubanov, S.; Tobin, M. J.; Cloetens, P.; Rosenhahn, A.; Lamb, R. N.; Luque, P.; Marchant, R.; Ivanova, E. P. Structure and Chemical Organization in Damselfly *Calopteryx haemorrhoidalis* Wings: A Spatially Resolved FTIR and XRF Analysis with Synchrotron Radiation. *Sci. Rep.* **2018**, *8* (1), 8413.

(43) Stainton, H. T. VI. Descriptions of Twenty-Five Species of Indian Micro-Lepidoptera. *Trans. R. Entomol. Soc. London* **1859**, *10* (3), 111–126.

(44) Ashton, R. XIV. On the Wings of the Hemiptera. *Ecol. Entomol.* **1842**, *3* (2), 95–98.

(45) Roonwal, M.; Verma, S.; Thakur, M. Evolution and systematic significance of wing microsculpturing in termites (Isoptera). V. Families Mastotermitidae, Termopsidae, Hodotermitidae and Stylotermitidae. *Proc. Indian Natl. Sci. Acad. B* **1979**, *115*–128.

(46) Findlay, G. Zoology. *J. R. Microsc. Soc.* **1933**, *53* (1), 39–59.

(47) Andrewes, H. XXXIX.—Papers on Oriental Carabidae.—XXII. *J. Nat. Hist.* **1929**, *4* (22), 353–371.

(48) Wagner, T.; Neinhuis, C.; Barthlott, W. Wettability and contaminability of insect wings as a function of their surface sculptures. *Acta Zool.* **1996**, *77* (3), 213–225.

(49) Kelleher, S. M.; Habimana, O.; Lawler, J.; O' Reilly, B.; Daniels, S.; Casey, E.; Cowley, A. Cicada Wing Surface Topography: An Investigation into the Bactericidal Properties of Nanostructural Features. *ACS Appl. Mater. Interfaces* **2016**, *8* (24), 14966–14974.

(50) Sun, M.; Watson, G. S.; Zheng, Y.; Watson, J. A.; Liang, A. Wetting properties on nanostructured surfaces of cicada wings. *J. Exp. Biol.* **2009**, *212* (19), 3148–3155.

(51) Selvakumar, R.; Karuppanan, K. K.; Pezhinkattil, R. Analysis on surface nanostructures present in hindwing of dragon fly (*Sympetrum vulgatum*) using atomic force microscopy. *Micron* **2012**, *43* (12), 1299–1303.

(52) Cheeseman, S.; Owen, S.; Truong, V. K.; Meyer, D.; Ng, S. H.; Vongsvivut, J.; Linklater, D.; Tobin, M. J.; Werner, M.; Baulin, V. A.; Luque, P.; Marchant, R.; Juodkazis, S.; Crawford, R. J.; Ivanova, E. P. Pillars of Life: Is There a Relationship between Lifestyle Factors and the Surface Characteristics of Dragonfly Wings? *ACS Omega* **2018**, *3* (6), 6039–6046.

(53) Watson, G. S.; Cribb, B. W.; Watson, J. A. How micro/nanoarchitecture facilitates anti-wetting: an elegant hierarchical design on the termite wing. *ACS Nano* **2010**, *4* (1), 129–136.

(54) Watson, G. S.; Green, D. W.; Cribb, B. W.; Brown, C. L.; Meritt, C. R.; Tobin, M. J.; Vongsvivut, J.; Sun, M.; Liang, A.-P.; Watson, J. A. Insect Analogue to the Lotus Leaf: A Planthopper Wing Membrane Incorporating a Low-Adhesion, Nonwetting, Superhydrophobic, Bactericidal, and Biocompatible Surface. *ACS Appl. Mater. Interfaces* **2017**, *9* (28), 24381–24392.

(55) Watson, G. S.; Myhra, S.; Cribb, B. W.; Watson, J. A. Putative functions and functional efficiency of ordered cuticular nanoarrays on insect wings. *Biophys. J.* **2008**, *94* (8), 3352–3360.

(56) Watson, G. S.; Watson, J. A. Natural nano-structures on insects—possible functions of ordered arrays characterized by atomic force microscopy. *Appl. Surf. Sci.* **2004**, *235* (1–2), 139–144.

(57) Watson, G. S.; Watson, J. A.; Cribb, B. W. Diversity of cuticular micro-and nanostructures on insects: Properties, functions, and potential applications. *Annu. Rev. Entomol.* **2017**, *62*, 185–205.

(58) Watson, G. S.; Watson, J. A.; Hu, S.; Brown, C. L.; Cribb, B.; Myhra, S. Micro and nanostructures found on insect wings—designs for minimising adhesion and friction. *Int. J. Nanomanuf.* **2010**, *5* (1–2), 112–128.

(59) Sun, M.; Liang, A.; Watson, G. S.; Watson, J. A.; Zheng, Y.; Ju, J.; Jiang, L. Influence of cuticle nanostructuring on the wetting behaviour/states on cicada wings. *PLoS One* **2012**, *7* (4), No. e35056.

(60) Li, X.-J.; Zhang, Z.-H.; Liang, Y.-H.; Ren, L.-Q.; Jie, M.; Yang, Z.-G. Antifatigue properties of dragonfly *Pantala flavescens* wings. *Microsc. Res. Tech.* **2014**, *77* (5), 356–362.

(61) Dirks, J.-H.; Taylor, D. Veins Improve Fracture Toughness of Insect Wings. *PLoS One* **2012**, *7* (8), No. e43411.

(62) Vance, J. T.; Roberts, S. P. The effects of artificial wing wear on the flight capacity of the honey bee *Apis mellifera*. *J. Insect Physiol.* **2014**, *65*, 27–36.

(63) Mountcastle, A. M.; Combes, S. A. Biomechanical strategies for mitigating collision damage in insect wings: structural design versus embedded elastic materials. *J. Exp. Biol.* **2014**, *217* (7), 1108–1115.

- (64) Shyy, W.; Kang, C.-k.; Chirarattananon, P.; Ravi, S.; Liu, H. Aerodynamics, sensing and control of insect-scale flapping-wing flight. *Proc. R. Soc. A* **2016**, *472* (2186), 20150712.
- (65) Karásek, M. Robotic hummingbird: Design of a control mechanism for a hovering flapping wing micro air vehicle. D. Eng. Sci. Thesis, Université Libre de Bruxelles, Brussels, Belgium, 2014.
- (66) Hill, R. W.; Wyse, G. A.; Anderson, M. *Animal Physiology*, 3rd ed.; Sinauer Associates: Sunderland, MA, 2012.
- (67) Collett, T.; Land, M. Visual control of flight behaviour in the hoverfly *Syrphoctonus pipiens* L. *J. Comp. Physiol., A* **1975**, *99* (1), 1–66.
- (68) Nachtigall, W. *Insects in flight: a glimpse behind the scenes in biophysical research*; McGraw-Hill: New York, 1974.
- (69) Dickinson, M. H.; Lehmann, F.-O.; Sane, S. P. Wing Rotation and the Aerodynamic Basis of Insect Flight. *Science* **1999**, *284* (5422), 1954–1960.
- (70) Ellington, C. P.; Van Den Berg, C.; Willmott, A. P.; Thomas, A. L. Leading-edge vortices in insect flight. *Nature* **1996**, *384* (6610), 626.
- (71) Chin, D. D.; Lentink, D. Flapping wing aerodynamics: from insects to vertebrates. *J. Exp. Biol.* **2016**, *219* (7), 920–932.
- (72) Dickinson, M. H.; Gotz, K. G. Unsteady aerodynamic performance of model wings at low Reynolds numbers. *J. Exp. Biol.* **1993**, *174* (1), 45–64.
- (73) Birch, J. M.; Dickinson, M. H. Spanwise flow and the attachment of the leading-edge vortex on insect wings. *Nature* **2001**, *412* (6848), 729.
- (74) Maxworthy, T. Experiments on the Weis-Fogh mechanism of lift generation by insects in hovering flight. Part 1. Dynamics of the 'fling'. *J. Fluid Mech.* **1979**, *93* (1), 47–63.
- (75) Weis-Fogh, T. Quick estimates of flight fitness in hovering animals, including novel mechanisms for lift production. *J. Exp. Biol.* **1973**, *59* (1), 169–230.
- (76) Bennett, L. Clap and fling aerodynamics—an experimental evaluation. *J. Exp. Biol.* **1977**, *69* (1), 261–272.
- (77) Sane, S. P.; Dickinson, M. H. The control of flight force by a flapping wing: lift and drag production. *J. Exp. Biol.* **2001**, *204* (15), 2607–2626.
- (78) Sane, S. P. The aerodynamics of insect flight. *J. Exp. Biol.* **2003**, *206* (23), 4191–4208.
- (79) Liu, L.; Sun, M. The added mass forces in insect flapping wings. *J. Theor. Biol.* **2018**, *437*, 45–50.
- (80) Wagner, H. Über die Entstehung des dynamischen Auftriebes von Tragflügeln. *Z. Angew. Math. Mech.* **1925**, *5* (1), 17–35.
- (81) Walker, P. Experiments on the growth of circulation about a wing and an apparatus for measuring fluid motion. *Rep. Memo. Aeronaut. Res. (Great Britain)* **1931**, 1402.
- (82) Whitney, J. P.; Wood, R. J. Aeromechanics of passive rotation in flapping flight. *J. Fluid Mech.* **2010**, *660*, 197–220.
- (83) Bomphrey, R. J.; Nakata, T.; Phillips, N.; Walker, S. M. Smart wing rotation and trailing-edge vortices enable high frequency mosquito flight. *Nature* **2017**, *544*, 92.
- (84) Rajabi, H.; Ghoroubi, N.; Stamm, K.; Appel, E.; Gorb, S. N. Dragonfly wing nodus: A one-way hinge contributing to the asymmetric wing deformation. *Acta Biomater.* **2017**, *60*, 330–338.
- (85) Zhang, S.; Sunami, Y.; Hashimoto, H. Deformation behavior of dragonfly-inspired nodus structured wing in gliding flight through experimental visualization approach. *Sci. Rep.* **2018**, *8* (1), 5751.
- (86) Wootton, R. J.; Evans, K. E.; Herbert, R.; Smith, C. W. The hind wing of the desert locust (*Schistocerca gregaria* Forskal). I. Functional morphology and mode of operation. *J. Exp. Biol.* **2000**, *203* (19), 2921–2931.
- (87) Wootton, R. J. Geometry and mechanics of insect hindwing fans—a modeling approach. *Proc. R. Soc. B* **1995**, *262* (1364), 181–187.
- (88) Ray, R. P.; Nakata, T.; Henningson, P.; Bomphrey, R. J. Enhanced flight performance by genetic manipulation of wing shape in *Drosophila*. *Nat. Commun.* **2016**, *7*, 10851.
- (89) Savage, N. Aerodynamics: Vortices and robobees. *Nature* **2015**, *521*, S64.
- (90) Floreano, D.; Wood, R. J. Science, technology and the future of small autonomous drones. *Nature* **2015**, *521*, 460.
- (91) Wood, R.; Nagpal, R.; Wei, G.-Y. Flight of the Robobees. *Sci. Am.* **2013**, *308* (3), 60–65.
- (92) Keennon, M.; Klingebiel, K.; Won, H. Development of the Nano Hummingbird: A Tailless Flapping Wing Micro Air Vehicle. In *50th AIAA Aerospace Sciences Meeting Including the New Horizons Forum and Aerospace Exposition*; American Institute of Aeronautics and Astronautics, 2012; DOI: 10.2514/6.2012-588.
- (93) de Croon, G. C.; Groen, M.; De Wagter, C.; Remes, B.; Ruijsink, R.; van Oudheusden, B. W. Design, aerodynamics and autonomy of the Delfly. *Bioinspiration Biomimetics* **2012**, *7* (2), 025003.
- (94) Pix, W.; Nalbach, G.; Zeil, J. Strepsipteran forewings are haltere-like organs of equilibrium. *Naturwissenschaften* **1993**, *80* (8), 371–374.
- (95) Cole, E. S.; Palka, J. The pattern of campaniform sensilla on the wing and haltere of *Drosophila melanogaster* and several of its homeotic mutants. *Development* **1982**, *71* (1), 41–61.
- (96) Hinson, B. T.; Morgansen, K. A. Gyroscopic sensing in the wings of the hawkmoth *Manduca sexta*: the role of sensor location and directional sensitivity. *Bioinspiration Biomimetics* **2015**, *10* (5), 056013.
- (97) Dickinson, M. H. Comparison of Encoding Properties of Campaniform sensilla on the Fly Wing. *J. Exp. Biol.* **1990**, *151* (1), 245–261.
- (98) Dickerson, B. H.; Aldworth, Z. N.; Daniel, T. L. Control of moth flight posture is mediated by wing mechanosensory feedback. *J. Exp. Biol.* **2014**, *217* (13), 2301–2308.
- (99) Pratt, B.; Deora, T.; Mohren, T.; Daniel, T. Neural evidence supports a dual sensory–motor role for insect wings. *Proc. R. Soc. London, Ser. B* **2017**, *284* (1862), 20170969.
- (100) Gettrup, E. Sensory Regulation of Wing Twisting in Locusts. *J. Exp. Biol.* **1966**, *44* (1), 1–16.
- (101) *Encyclopedia of Insects*, 2nd ed.; Resh, V. H., Cardé, R. T., Eds.; Academic Press: San Diego, 2009.
- (102) Kingsolver, J. G.; Koehl, M. A. R. Aerodynamics, thermoregulation, and the evolution of insect wings: Differential scaling and evolutionary change. *Evolution* **1985**, *39* (3), 488–504.
- (103) Douglas, M. M. Thermoregulatory significance of thoracic lobes in the evolution of insect wings. *Science* **1981**, *211* (4477), 84–86.
- (104) Narasimhan, V.; Siddique, R. H.; Lee, J. O.; Kumar, S.; Ndjamien, B.; Du, J.; Hong, N.; Sretavan, D.; Choo, H. Multifunctional biophotonic nanostructures inspired by the longtail glasswing butterfly for medical devices. *Nat. Nanotechnol.* **2018**, *13* (6), 512–519.
- (105) Callahan, P. S. Insect antennae with special reference to the mechanism of scent detection and the evolution of the sensilla. *Int. J. Insect Morphol. Embryol.* **1975**, *4* (5), 381–430.
- (106) Schneider, D. Insect antennae. *Annu. Rev. Entomol.* **1964**, *9* (1), 103–122.
- (107) Sane, S. P.; Dieudonné, A.; Willis, M. A.; Daniel, T. L. Antennal mechanosensors mediate flight control in moths. *Science* **2007**, *315* (5813), 863–866.
- (108) Fuller, S. B.; Straw, A. D.; Peek, M. Y.; Murray, R. M.; Dickinson, M. H. Flying *Drosophila* stabilize their vision-based velocity controller by sensing wind with their antennae. *Proc. Natl. Acad. Sci. U. S. A.* **2014**, *111*, E1182–E1191.
- (109) Yao, X.; Song, Y.; Jiang, L. Applications of bio-inspired special wettable surfaces. *Adv. Mater.* **2011**, *23* (6), 719–734.
- (110) Gittens, R. A.; Scheideler, L.; Rupp, F.; Hyzy, S. L.; Geis-Gerstorfer, J.; Schwartz, Z.; Boyan, B. D. A review on the wettability of dental implant surfaces II: biological and clinical aspects. *Acta Biomater.* **2014**, *10* (7), 2907–2918.
- (111) Meiron, T.; Saguy, I. Wetting properties of food packaging. *Food Res. Int.* **2007**, *40* (5), 653–659.
- (112) Morrow, N. R. Wettability and its effect on oil recovery. *JPT, J. Pet. Technol.* **1990**, *42* (12), 1476–1484.

- (113) Wagner, T.; Neinhuis, C.; Barthlott, W. Wettability and contaminability of insect wings as a function of their surface sculptures. *Acta Zool.* **1996**, *77* (3), 213–225.
- (114) Cassie, A.; Baxter, S. Wettability of porous surfaces. *Trans. Faraday Soc.* **1944**, *40*, 546–551.
- (115) Lafuma, A.; Quéré, D. Superhydrophobic states. *Nat. Mater.* **2003**, *2* (7), 457.
- (116) Byun, D.; Hong, J.; Saputra, Ko, J. H.; Lee, Y. J.; Park, H. C.; Byun, B.-K.; Lukes, J. R. Wetting characteristics of insect wing surfaces. *J. Bionic Eng.* **2009**, *6* (1), 63–70.
- (117) Oh, J.; Dana, C. E.; Hong, S.; Roman, J. K.; Jo, K. D.; Hong, J. W.; Nguyen, J.; Cropek, D. M.; Alleyne, M.; Miljkovic, N. Exploring the role of habitat on the wettability of cicada wings. *ACS Appl. Mater. Interfaces* **2017**, *9* (32), 27173–27184.
- (118) Hasan, J.; Webb, H. K.; Truong, V. K.; Watson, G. S.; Watson, J. A.; Tobin, M. J.; Gervinskas, G.; Juodkazy, S.; Wang, J. Y.; Crawford, R. J.; Ivanova, E. P. Spatial variations and temporal metastability of the self-cleaning and superhydrophobic properties of damselfly wings. *Langmuir* **2012**, *28* (50), 17404–17409.
- (119) Zheng, Y.; Gao, X.; Jiang, L. Directional adhesion of superhydrophobic butterfly wings. *Soft Matter* **2007**, *3* (2), 178–182.
- (120) Watson, G. S.; Cribb, B. W.; Watson, J. A. Contrasting micro/nano architecture on termite wings: two divergent strategies for optimizing success of colonisation flights. *PLoS One* **2011**, *6* (9), No. e24368.
- (121) Sun, M.; Liang, A.; Watson, G. S.; Watson, J. A.; Zheng, Y.; Jiang, L. Compound microstructures and wax layer of beetle elytral surfaces and their influence on wetting properties. *PLoS One* **2012**, *7* (10), No. e46710.
- (122) Hu, H.-M. S.; Watson, G. S.; Cribb, B. W.; Watson, J. A. Non-wetting wings and legs of the crane fly aided by fine structures of the cuticle. *J. Exp. Biol.* **2011**, *214* (6), 915–920.
- (123) Watson, G. S.; Cribb, B. W.; Watson, J. A. The role of micro/nano channel structuring in repelling water on cuticle arrays of the lacewing. *J. Struct. Biol.* **2010**, *171* (1), 44–51.
- (124) Sun, G.; Fang, Y.; Cong, Q.; Ren, L.-q. Anisotropism of the Non-Smooth Surface of Butterfly Wing. *J. Bionic Eng.* **2009**, *6* (1), 71–76.
- (125) Bixler, G. D.; Bhushan, B. Bioinspired rice leaf and butterfly wing surface structures combining shark skin and lotus effects. *Soft Matter* **2012**, *8* (44), 11271–11284.
- (126) Han, J. T.; Kim, S.; Karim, A. UVO-tunable superhydrophobic to superhydrophilic wetting transition on biomimetic nanostructured surfaces. *Langmuir* **2007**, *23* (5), 2608–2614.
- (127) Lee, Y.; Yoo, Y.; Kim, J.; Widhiarini, S.; Park, B.; Park, H. C.; Yoon, K. J.; Byun, D. Mimicking a Superhydrophobic Insect Wing by Argon and Oxygen Ion Beam Treatment on Polytetrafluoroethylene Film. *J. Bionic Eng.* **2009**, *6* (4), 365–370.
- (128) Liang, F.; Lehr, J.; Danielczak, L.; Leask, R.; Kietzig, A. M. Robust Non-Wetting PTFE Surfaces by Femtosecond Laser Machining. *Int. J. Mol. Sci.* **2014**, *15* (8), 13681–13696.
- (129) Liu, Z. J.; Wang, H. Y.; Zhang, X. G.; Wang, C. J.; Lv, C. J.; Zhu, Y. J. Durable and self-healing superhydrophobic surface with bistratal gas layers prepared by electrospinning and hydrothermal processes. *Chem. Eng. J.* **2017**, *326*, 578–586.
- (130) Vukusic, P.; Sambles, J. R.; Lawrence, C. R.; Wootton, R. J. Quantified interference and diffraction in single Morpho butterfly scales. *Proc. R. Soc. B* **1999**, *266* (1427), 1403–1411.
- (131) Vukusic, P.; Sambles, J. R.; Lawrence, C. R. Colour mixing in wing scales of a butterfly. *Nature* **2000**, *404*, 457.
- (132) Kolle, M.; Salgard-Cunha, P. M.; Scherer, M. R.; Huang, F.; Vukusic, P.; Mahajan, S.; Baumberg, J. J.; Steiner, U. Mimicking the colourful wing scale structure of the Papilio blumei butterfly. *Nat. Nanotechnol.* **2010**, *5* (7), 511–5.
- (133) Han, Z.; Mu, Z.; Li, B.; Niu, S.; Zhang, J.; Ren, L. A High-Transmission, Multiple Antireflective Surface Inspired from Bilayer 3D Ultrafine Hierarchical Structures in Butterfly Wing Scales. *Small* **2016**, *12* (6), 713–20.
- (134) Siddique, R. H.; Vignolini, S.; Bartels, C.; Wacker, I.; Hölscher, H. Colour formation on the wings of the butterfly *Hypolimnas salmactis* by scale stacking. *Sci. Rep.* **2016**, *6*, 36204.
- (135) Siddique, R. H.; Donie, Y. J.; Gomard, G.; Yalamanchili, S.; Merdzhanova, T.; Lemmer, U.; Hölscher, H. J. Bioinspired phase-separated disordered nanostructures for thin photovoltaic absorbers. *Sci. Adv.* **2017**, *3* (10), e1700232.
- (136) Ge, D.; Wu, G.; Yang, L.; Kim, H.-N.; Hallwachs, W.; Burns, J. M.; Janzen, D. H.; Yang, S. Varying and unchanging whiteness on the wings of dusk-active and shade-inhabiting Carystoides escalantei butterflies. *Proc. Natl. Acad. Sci. U. S. A.* **2017**, *114* (28), 7379–7384.
- (137) Stavenga, D. G. Thin Film and Multilayer Optics Cause Structural Colors of Many Insects and Birds. *Mater. Today: Proc.* **2014**, *1*, 109–121.
- (138) Zhang, D.; Zhang, W.; Gu, J.; Fan, T.; Liu, Q.; Su, H.; Zhu, S. Inspiration from butterfly and moth wing scales: Characterization, modeling, and fabrication. *Prog. Mater. Sci.* **2015**, *68*, 67–96.
- (139) Huang, J.; Wang, X.; Wang, Z. L. Controlled replication of butterfly wings for achieving tunable photonic properties. *Nano Lett.* **2006**, *6* (10), 2325–2331.
- (140) Phillip, R. W.; Bleikolm, A. F. J. A. O. *Appl. Opt.* **1996**, *35* (28), 5529–5534.
- (141) England, G.; Kolle, M.; Kim, P.; Khan, M.; Munoz, P.; Mazur, E.; Aizenberg, J. Bioinspired micrograting arrays mimicking the reverse color diffraction elements evolved by the butterfly Pierella luna. *Proc. Natl. Acad. Sci. U. S. A.* **2014**, *111* (44), 15630–4.
- (142) Zhou, H.; Xu, J.; Liu, X.; Zhang, H.; Wang, D.; Chen, Z.; Zhang, D.; Fan, T. Bio-Inspired Photonic Materials: Prototypes and Structural Effect Designs for Applications in Solar Energy Manipulation. *Adv. Funct. Mater.* **2018**, *28* (24), 1705309.
- (143) Chattopadhyay, S.; Huang, Y. F.; Jen, Y. J.; Ganguly, A.; Chen, K. H.; Chen, L. C. Anti-reflecting and photonic nanostructures. *Mater. Sci. Eng., R* **2010**, *69* (1–3), 1–35.
- (144) Sun, M.; Liang, A.; Zheng, Y.; Watson, G. S.; Watson, J. A. A study of the anti-reflection efficiency of natural nano-arrays of varying sizes. *Bioinspiration Biomimetics* **2011**, *6* (2), 026003.
- (145) Yu, K.; Fan, T.; Lou, S.; Zhang, D. Biomimetic optical materials: Integration of nature's design for manipulation of light. *Prog. Mater. Sci.* **2013**, *58* (6), 825–873.
- (146) Zada, I.; Zhang, W.; Li, Y.; Sun, P.; Cai, N.; Gu, J.; Liu, Q.; Su, H.; Zhang, D. Angle dependent antireflection property of TiO₂ inspired by cicada wings. *Appl. Phys. Lett.* **2016**, *109* (15), 153701.
- (147) Zada, I.; Zhang, W.; Sun, P.; Imtiaz, M.; Abbas, W.; Zhang, D. Multifunctional, angle dependent antireflection, and hydrophilic properties of SiO₂ inspired by nano-scale structures of cicada wings. *Appl. Phys. Lett.* **2017**, *111* (15), 153701.
- (148) Potyrailo, R. A.; Bonam, R. K.; Hartley, J. G.; Starkey, T. A.; Vukusic, P.; Vasudev, M.; Bunning, T.; Naik, R. R.; Tang, Z.; Palacios, M. A.; Larsen, M.; Le Tarte, L. A.; Grande, J. C.; Zhong, S.; Deng, T. Towards outperforming conventional sensor arrays with fabricated individual photonic vapour sensors inspired by Morpho butterflies. *Nat. Commun.* **2015**, *6*, 7959.
- (149) Jiang, T.; Peng, Z.; Wu, W.; Shi, T.; Liao, G. Gas sensing using hierarchical micro/nanostructures of Morpho butterfly scales. *Sens. Actuators, A* **2014**, *213*, 63–69.
- (150) Potyrailo, R. A.; Ghiradella, H.; Vertiatichik, A.; Dovidenko, K.; Cournoyer, J. R.; Olson, E. J. Morpho butterfly wing scales demonstrate highly selective vapour response. *Nat. Photonics* **2007**, *1* (2), 123–128.
- (151) Potyrailo, R. A.; Starkey, T. A.; Vukusic, P.; Ghiradella, H.; Vasudev, M.; Bunning, T.; Naik, R. R.; Tang, Z.; Larsen, M.; Deng, T.; Zhong, S.; Palacios, M.; Grande, J. C.; Zorn, G.; Goddard, G.; Zalubovsky, S. Discovery of the surface polarity gradient on iridescent Morpho butterfly scales reveals a mechanism of their selective vapor response. *Proc. Natl. Acad. Sci. U. S. A.* **2013**, *110* (39), 15567–72.
- (152) Eadie, L.; Ghosh, T. K. Biomimicry in textiles: past, present and potential. An overview. *J. R. Soc., Interface* **2011**, *8* (59), 761–75.

- (153) Zhang, S.; Chen, Y. Nanofabrication and coloration study of artificial Morpho butterfly wings with aligned lamellae layers. *Sci. Rep.* **2015**, *5*, 16637.
- (154) Rodriguez, R. E.; Agarwal, S. P.; An, S.; Kazyak, E.; Das, D.; Shang, W.; Skye, R.; Deng, T.; Dasgupta, N. P. Biotemplated Morpho Butterfly Wings for Tunable Structurally Colored Photocatalysts. *ACS Appl. Mater. Interfaces* **2018**, *10* (5), 4614–4621.
- (155) Han, Z.; Yang, M.; Li, B.; Mu, Z.; Niu, S.; Zhang, J.; Yang, X. Excellent Color Sensitivity of Butterfly Wing Scales to Liquid Mediums. *J. Bionic Eng.* **2016**, *13* (3), 355–363.
- (156) Regan, E. C.; Shen, Y.; Lopez, J. J.; Hsu, C. W.; Zhen, B.; Joannopoulos, J. D.; Soljačić, M. Substrate-independent light confinement in bioinspired all-dielectric surface resonators. *ACS Photonics* **2016**, *3* (4), 532–536.
- (157) Lal, N. N.; Le, K. N.; Thomson, A. F.; Brauers, M.; White, T. P.; Catchpole, K. R. Transparent Long-Pass Filter with Short-Wavelength Scattering Based on Morpho Butterfly Nanostructures. *ACS Photonics* **2017**, *4* (4), 741–745.
- (158) Krishna, A.; Lee, J. Morphology-Driven Emissivity of Microscale Tree-like Structures for Radiative Thermal Management. *Nanoscale Microscale Thermophys. Eng.* **2018**, *22* (2), 124–136.
- (159) Wijnen, B.; Leertouwer, H. L.; Stavenga, D. G. Colors and pterin pigmentation of pierid butterfly wings. *J. Insect Physiol.* **2007**, *53* (12), 1206–17.
- (160) Niu, S.; Li, B.; Mu, Z.; Yang, M.; Zhang, J.; Han, Z.; Ren, L. Excellent Structure-Based Multifunction of Morpho Butterfly Wings: A Review. *J. Bionic Eng.* **2015**, *12* (2), 170–189.
- (161) Liu, F.; Liu, Y.; Huang, L.; Hu, X.; Dong, B.; Shi, W.; Xie, Y.; Ye, X. Replication of homologous optical and hydrophobic features by templating wings of butterflies Morpho menelaus. *Opt. Commun.* **2011**, *284* (9), 2376–2381.
- (162) Saito, A. Material design and structural color inspired by biomimetic approach. *Sci. Technol. Adv. Mater.* **2011**, *12* (6), 064709.
- (163) Saito, A.; Miyamura, Y.; Nakajima, M.; Ishikawa, Y.; Sogo, K.; Kuwahara, Y.; Hirai, Y. Reproduction of the Morpho blue by nanocasting lithography. *J. Vac. Sci. Technol., B: Nanotechnol. Microelectron.: Mater., Process., Meas., Phenom.* **2006**, *24* (6), 3248–3251.
- (164) Vigneron, J. P.; Simonis, P.; Aiello, A.; Bay, A.; Windsor, D. M.; Colomer, J.-F.; Rassart, M. Reverse color sequence in the diffraction of white light by the wing of the male butterfly *Pierella luna* (Nymphalidae: Satyrinae). *Phys. Rev. E* **2010**, *82* (2), 021903.
- (165) Shevtsova, E.; Hansson, C.; Janzen, D. H.; Kjaerandsen, J. Stable structural color patterns displayed on transparent insect wings. *Proc. Natl. Acad. Sci. U. S. A.* **2011**, *108* (2), 668–73.
- (166) Siddique, R. H.; Gomard, G.; Hölscher, H. The role of random nanostructures for the omnidirectional anti-reflection properties of the glasswing butterfly. *Nat. Commun.* **2015**, *6*, 6909.
- (167) Zhao, Q.; Guo, X.; Fan, T.; Ding, J.; Zhang, D.; Guo, Q. Art of blackness in butterfly wings as natural solar collector. *Soft Matter* **2011**, *7* (24), 11433–11439.
- (168) Xie, G.; Zhang, G.; Lin, F.; Zhang, J.; Liu, Z.; Mu, S. The fabrication of subwavelength anti-reflective nanostructures using a bio-temple. *Nanotechnology* **2008**, *19* (9), 095605.
- (169) Xie, H.; Huang, H. X.; Peng, Y. J. Rapid fabrication of bio-inspired nanostructure with hydrophobicity and antireflectivity on polystyrene surface replicating from cicada wings. *Nanoscale* **2017**, *9* (33), 11951–11958.
- (170) Kostovski, G.; White, D. J.; Mitchell, A.; Austin, M. W.; Stoddart, P. R. Nanoimprinted optical fibres: Biotemplated nanostructures for SERS sensing. *Biosens. Bioelectron.* **2009**, *24* (5), 1531–1535, DOI: [10.1016/j.bios.2008.10.016](https://doi.org/10.1016/j.bios.2008.10.016).
- (171) Tripathy, A.; Sen, P. Dragonfly wing inspired multifunctional antireflective superhydrophobic surfaces. In *2016 Third International Conference on Emerging Electronics (ICEE)*; IEEE, 2016; pp 1–3.
- (172) Yoshida, A.; Motoyama, M.; Kosaku, A.; Miyamoto, K. Antireflective nanoprotuberance array in the transparent wing of a hawkmoth, *Cephonodes hylas*. *Zool. Sci.* **1997**, *14* (5), 737–741.
- (173) Hooper, I. R.; Vukusic, P.; Wootton, R. J. Detailed optical study of the transparent wing membranes of the dragonfly *Aeshna cyanea*. *Opt. Express* **2006**, *14* (11), 4891–4897.
- (174) Hasan, J.; Crawford, R. J.; Ivanova, E. P. Antibacterial surfaces: the quest for a new generation of biomaterials. *Trends Biotechnol.* **2013**, *31* (5), 295–304.
- (175) Elbourne, A.; Crawford, R. J.; Ivanova, E. P. Nano-structured antimicrobial surfaces: From nature to synthetic analogues. *J. Colloid Interface Sci.* **2017**, *508*, 603–616.
- (176) Bandara, C. D.; Singh, S.; Afara, I. O.; Wolff, A.; Tesfamichael, T.; Ostrikov, K.; Oloyede, A. Bactericidal Effects of Natural Nanotopography of Dragonfly Wing on *Escherichia coli*. *ACS Appl. Mater. Interfaces* **2017**, *9* (8), 6746–6760.
- (177) Hasan, J.; Webb, H. K.; Truong, V. K.; Pogodin, S.; Baulin, V. A.; Watson, G. S.; Watson, J. A.; Crawford, R. J.; Ivanova, E. P. Selective bactericidal activity of nanopatterned superhydrophobic cicada Psaltoda claripennis wing surfaces. *Appl. Microbiol. Biotechnol.* **2013**, *97* (20), 9257–9262.
- (178) Ivanova, E. P.; Hasan, J.; Webb, H. K.; Truong, V. K.; Watson, G. S.; Watson, J. A.; Baulin, V. A.; Pogodin, S.; Wang, J. Y.; Tobin, M. J.; Lötbe, C.; Crawford, R. J. Natural Bactericidal Surfaces: Mechanical Rupture of Pseudomonas aeruginosa Cells by Cicada Wings. *Small* **2012**, *8* (16), 2489–2494.
- (179) Pogodin, S.; Hasan, J.; Baulin, V. A.; Webb, H. K.; Truong, V. K.; Nguyen, T. H. P.; Boshkovik, V.; Fluke, C. J.; Watson, G. S.; Watson, J. A.; Crawford, R. J.; Ivanova, E. P. Biophysical Model of Bacterial Cell Interactions with Nanopatterned Cicada Wing Surfaces. *Biophys. J.* **2013**, *104* (4), 835–840.
- (180) Truong, V. K.; Geeganagamage, N. M.; Baulin, V. A.; Vongsvivut, J.; Tobin, M. J.; Luque, P.; Crawford, R. J.; Ivanova, E. P. The susceptibility of *Staphylococcus aureus* CIP 65.8 and *Pseudomonas aeruginosa* ATCC 9721 cells to the bactericidal action of nano-structured *Calopteryx haemorrhoidalis* damselfly wing surfaces. *Appl. Microbiol. Biotechnol.* **2017**, *101* (11), 4683–4690.
- (181) Mainwaring, D. E.; Nguyen, S. H.; Webb, H.; Jakubov, T.; Tobin, M.; Lamb, R. N.; Wu, A. H. F.; Marchant, R.; Crawford, R. J.; Ivanova, E. P. The nature of inherent bactericidal activity: insights from the nanotopology of three species of dragonfly. *Nanoscale* **2016**, *8* (12), 6527–6534.
- (182) Ivanova, E. P.; Nguyen, S. H.; Guo, Y.; Baulin, V. A.; Webb, H. K.; Truong, V. K.; Wandiyanto, J. V.; Garvey, C. J.; Mahon, P. J.; Mainwaring, D. E.; Crawford, R. J. Bactericidal activity of self-assembled palmitic and stearic fatty acid crystals on highly ordered pyrolytic graphite. *Acta Biomater.* **2017**, *59*, 148–157.
- (183) Hasan, J.; Chatterjee, K. Recent advances in engineering topography mediated antibacterial surfaces. *Nanoscale* **2015**, *7* (38), 15568–15575.
- (184) Pham, V. T.; Truong, V. K.; Orlowska, A.; Ghanaati, S.; Barbeck, M.; Booms, P.; Fulcher, A. J.; Bhadra, C. M.; Buividas, R.; Baulin, V.; Kirkpatrick, C. J.; Doran, P.; Mainwaring, D. E.; Juodkazis, S.; Crawford, R. J.; Ivanova, E. P. “Race for the Surface”: Eukaryotic Cells Can Win. *ACS Appl. Mater. Interfaces* **2016**, *8* (34), 22025–31.
- (185) Hasan, J.; Jain, S.; Chatterjee, K. Nanoscale Topography on Black Titanium Imparts Multi-biofunctional Properties for Orthopedic Applications. *Sci. Rep.* **2017**, *7*, 41118.
- (186) Ivanova, E. P.; Hasan, J.; Webb, H. K.; Gervinskas, G.; Juodkazis, S.; Truong, V. K.; Wu, A. H. F.; Lamb, R. N.; Baulin, V. A.; Watson, G. S.; Watson, J. A.; Mainwaring, D. E.; Crawford, R. J. Bactericidal activity of black silicon. *Nat. Commun.* **2013**, *4*, 2838.
- (187) Diu, T.; Faruqi, N.; Sjöström, T.; Lamarre, B.; Jenkinson, H. F.; Su, B.; Ryadnov, M. G. Cicada-inspired cell-instructive nano-patterned arrays. *Sci. Rep.* **2015**, *4* (1), 7122.
- (188) Hasan, J.; Raj, S.; Yadav, L.; Chatterjee, K. Engineering a nanostructured “super surface” with superhydrophobic and super-killing properties. *RSC Adv.* **2015**, *5* (56), 44953–44959.
- (189) Bhadra, C. M.; Werner, M.; Baulin, V. A.; Truong, V. K.; Al Kobaisi, M.; Nguyen, S. H.; Balcytis, A.; Juodkazis, S.; Wang, J. Y.; Mainwaring, D. E.; Crawford, R. J.; Ivanova, E. P. Subtle Variations in

Surface Properties of Black Silicon Surfaces Influence the Degree of Bactericidal Efficiency. *Nano-Micro Lett.* **2018**, *10* (2), 36.

(190) Hasan, J.; Jain, S.; Padmarajan, R.; Purighalla, S.; Sambandamurthy, V. K.; Chatterjee, K. Multi-scale surface topography to minimize adherence and viability of nosocomial drug-resistant bacteria. *Mater. Des.* **2018**, *140*, 332–344.

(191) Tripathy, A.; Kumar, A.; Chowdhury, A. R.; Karmakar, K.; Purighalla, S.; Sambandamurthy, V.; Chakravorty, D.; Sen, P. A Nanowire-Based Flexible Antibacterial Surface Reduces the Viability of Drug-Resistant Nosocomial Pathogens. *ACS Applied Nano Materials* **2018**, *1* (6), 2678–2688.

(192) Wang, X.; Bhadra, C. M.; Yen Dang, T. H.; Buividas, R.; Wang, J.; Crawford, R. J.; Ivanova, E. P.; Juodkakis, S. A bactericidal microfluidic device constructed using nano-textured black silicon. *RSC Adv.* **2016**, *6* (31), 26300–26306.

(193) Jaggesar, A.; Mathew, A.; Wang, H.; Tesfamichael, T.; Yan, C.; Yarlagadda, P. K. D. V. Mechanical, bactericidal and osteogenic behaviours of hydrothermally synthesised TiO₂ nanowire arrays. *J. Mech. Behav. Biomed. Mater.* **2018**, *80*, 311–319.

(194) Linklater, D. P.; De Volder, M.; Baulin, V. A.; Werner, M.; Jessl, S.; Golozar, M.; Maggini, L.; Rubanov, S.; Hanssen, E.; Juodkakis, S.; Ivanova, E. P. High Aspect Ratio Nanostructures Kill Bacteria via Storage and Release of Mechanical Energy. *ACS Nano* **2018**, *12* (7), 6657–6667.

(195) Jaggesar, A.; Shahali, H.; Mathew, A.; Yarlagadda, P. K. D. V. Bio-mimicking nano and micro-structured surface fabrication for antibacterial properties in medical implants. *J. Nanobiotechnol.* **2017**, *15* (1), 64.

(196) Lutey, A. H. A.; Gemini, L.; Romoli, L.; Lazzini, G.; Fuso, F.; Faucon, M.; Kling, R. Towards Laser-Textured Antibacterial Surfaces. *Sci. Rep.* **2018**, *8* (1), 10112.

(197) Liu, H. Integrated modeling of insect flight: from morphology, kinematics to aerodynamics. *J. Comput. Phys.* **2009**, *228* (2), 439–459.

(198) Wood, R. J. Liftoff of a 60mg flapping-wing MAV. In *2007 IEEE/RJS International Conference on Intelligent Robots and Systems (IROS 2007)*; IEEE, 2007; pp 1889–1894.

(199) Dudley, R.; Ellington, C. P. Mechanics of forward flight in bumblebees: II. Quasi-steady lift and power requirements. *J. Exp. Biol.* **1990**, *148* (1), 53–88.

(200) Dickinson, M. The effects of wing rotation on unsteady aerodynamic performance at low Reynolds numbers. *J. Exp. Biol.* **1994**, *192* (1), 179–206.

(201) Ansari, S. A.; Żbikowski, R.; Knowles, K. Non-linear unsteady aerodynamic model for insect-like flapping wings in the hover. Part 1: Methodology and analysis. *Proc. Inst. Mech. Eng., Part G* **2006**, *220* (2), 61–83.

(202) Ansari, S. A.; Żbikowski, R.; Knowles, K. Non-linear unsteady aerodynamic model for insect-like flapping wings in the hover. Part 2: Implementation and validation. *Proc. Inst. Mech. Eng., Part G* **2006**, *220* (3), 169–186.

(203) Berman, G. J.; Wang, Z. J. Energy-minimizing kinematics in hovering insect flight. *J. Fluid Mech.* **2007**, *582*, 153–168.

(204) Armanini, S. F.; Caetano, J. V.; Croon, G. C. H. E. d.; Visser, C. C. d.; Mulder, M. Quasi-steady aerodynamic model of clap-and-fling flapping MAV and validation using free-flight data. *Bioinspiration Biomimetics* **2016**, *11* (4), 046002.

(205) Sane, S. P.; Dickinson, M. H. The aerodynamic effects of wing rotation and a revised quasi-steady model of flapping flight. *J. Exp. Biol.* **2002**, *205* (8), 1087–1096.

(206) Wang, Q.; Goosen, J.; van Keulen, F. A predictive quasi-steady model of aerodynamic loads on flapping wings. *J. Fluid Mech.* **2016**, *800*, 688–719.

(207) Shyy, W.; Aono, H.; Chimakurthi, S. K.; Trizila, P.; Kang, C.-K.; Cesnik, C. E.; Liu, H. Recent progress in flapping wing aerodynamics and aeroelasticity. *Prog. Aerosp. Sci.* **2010**, *46* (7), 284–327.

(208) Nakata, T.; Liu, H. Aerodynamic performance of a hovering hawkmoth with flexible wings: a computational approach. *Proc. R. Soc. London, Ser. B* **2012**, *279*, 722–731.

(209) Nakata, T.; Noda, R.; Liu, H. Fluid–structure interaction enhances the aerodynamic performance of flapping wings: a computational study. *J. Biomech. Sci. Eng.* **2018**, *13* (2), 17-006666.

(210) Aono, H.; Liang, F.; Liu, H. Near-and far-field aerodynamics in insect hovering flight: an integrated computational study. *J. Exp. Biol.* **2008**, *211* (2), 239–257.

(211) Wang, Z. J. The role of drag in insect hovering. *J. Exp. Biol.* **2004**, *207* (23), 4147–4155.

(212) Wang, Z. J.; Birch, J. M.; Dickinson, M. H. Unsteady forces and flows in low Reynolds number hovering flight: two-dimensional computations vs robotic wing experiments. *J. Exp. Biol.* **2004**, *207* (3), 449–460.

(213) Santhanakrishnan, A.; Jones, S. K.; Dickson, W. B.; Peek, M.; Kasoju, V. T.; Dickinson, M. H.; Miller, L. A. Flow Structure and Force Generation on Flapping Wings at Low Reynolds Numbers Relevant to the Flight of Tiny Insects. *Fluids* **2018**, *3* (3), 45.

(214) Moses, K. C.; Prigg, D.; Weisfeld, M.; Bachmann, R. J.; Willis, M.; Quinn, R. D. Simulating Flapping Wing Mechanisms Inspired by the *Manduca sexta* Hawkmoth. *Lect. Notes Comput. Sci.* **2018**, *10928*, 326–337.

(215) Aono, H.; Liang, F.; Liu, H. Near- and far-field aerodynamics in insect hovering flight: an integrated computational study. *J. Exp. Biol.* **2008**, *211* (2), 239–257.

(216) Li, X. Bactericidal mechanism of nanopatterned surfaces. *Phys. Chem. Chem. Phys.* **2016**, *18* (2), 1311–1316.

(217) Ye, Z.; Kim, A.; Mottley, C. Y.; Ellis, M. W.; Wall, C.; Esker, A. R.; Nain, A. S.; Behkam, B. Design of Nanofiber Coatings for Mitigation of Microbial Adhesion: Modeling and Application to Medical Catheters. *ACS Appl. Mater. Interfaces* **2018**, *10* (18), 15477–15486.

(218) Pogodin, S.; Baulin, V. A. Coarse-grained models of phospholipid membranes within the single chain mean field theory. *Soft Matter* **2010**, *6* (10), 2216–2226.

(219) Pornsin-Sirirak, T. N.; Lee, S. W.; Nassef, H.; Grasmeyer, J.; Tai, Y. C.; Ho, C. M.; Keennon, M. MEMS wing technology for a battery-powered ornithopter. In *Proceedings of the IEEE 13th Annual International Conference on Micro Electro Mechanical Systems (MEMS 2000)*; IEEE, 2000; pp 799–804.

(220) DeLaurier, J. D.; Harris, J. M. A study of mechanical flapping-wing flight. *Aeronaut. J.* **1993**, *97* (968), 277–286.

(221) Takahashi, H.; Aoyama, Y.; Ohsawa, K.; Tanaka, H.; Iwase, E.; Matsumoto, K.; Shimoyama, I. Differential pressure measurement using a free-flying insect-like ornithopter with an MEMS sensor. *Bioinspiration Biomimetics* **2010**, *5* (3), 036005.

(222) Tanaka, H.; Wood, R. J. Fabrication of corrugated artificial insect wings using laser micromachined molds. *J. Micromech. Microeng.* **2010**, *20* (7), 075008.

(223) Tanaka, H.; Matsumoto, K.; Shimoyama, I. Fabrication of a three-dimensional insect-wing model by micromolding of thermosetting resin with a thin elastomeric mold. *J. Micromech. Microeng.* **2007**, *17* (12), 2485.

(224) Zhang, G.; Zhang, J.; Xie, G.; Liu, Z.; Shao, H. Cicada wings: a stamp from nature for nanoimprint lithography. *Small* **2006**, *2* (12), 1440–1443.

(225) Shang, J.; Combes, S. A.; Finio, B.; Wood, R. J. Artificial insect wings of diverse morphology for flapping-wing micro air vehicles. *Bioinspiration Biomimetics* **2009**, *4* (3), 036002.

(226) Ko, J. H.; Kim, J.; Hong, J.; Yoo, Y.; Lee, Y.; Jin, T. L.; Park, H. C.; Goo, N. S.; Byun, D. Micro/nanofabrication for a realistic beetle wing with a superhydrophobic surface. *Bioinspiration Biomimetics* **2012**, *7* (1), 016011.

(227) Hong, S.-H.; Hwang, J.; Lee, H. Replication of cicada wing's nano-patterns by hot embossing and UV nanoimprinting. *Nano-technology* **2009**, *20* (38), 385303.

(228) Narasimhan, V.; Siddique, R. H.; Lee, J. O.; Kumar, S.; Ndjamen, B.; Du, J.; Hong, N.; Sretavan, D.; Choo, H. Multifunc-

tional biophotonic nanostructures inspired by the longtail glasswing butterfly for medical devices. *Nat. Nanotechnol.* **2018**, *13* (6), 512–519.

(229) Hasan, J.; Jain, S.; Padmarajan, R.; Purighalla, S.; Sambandamurthy, V.; Chatterjee, K. Multi-scale surface topography to minimize adherence and viability of nosocomial drug-resistant bacteria. *Mater. Des.* **2018**, *140*, 332–344.

(230) Wang, X.; Song, W.; Li, Z.; Cong, Q. Fabrication of superhydrophobic AAO-Ag multilayer mimicking dragonfly wings. *Chin. Sci. Bull.* **2012**, *57* (35), 4635–4640.

(231) Ivanova, E. P.; Hasan, J.; Webb, H. K.; Truong, V. K.; Watson, G. S.; Watson, J. A.; Baulin, V. A.; Pogodin, S.; Wang, J. Y.; Tobin, M. J.; Lobbé, C.; Crawford, R. J. Natural bactericidal surfaces: mechanical rupture of *Pseudomonas aeruginosa* cells by cicada wings. *Small* **2012**, *8* (16), 2489–2494.

(232) Tan, Y.; Gu, J.; Zang, X.; Xu, W.; Shi, K.; Xu, L.; Zhang, D. Versatile fabrication of intact three-dimensional metallic butterfly wing scales with hierarchical sub-micrometer structures. *Angew. Chem., Int. Ed.* **2011**, *50* (36), 8307–11.

(233) Lo, M.-L.; Li, W.-H.; Tseng, S.-Z.; Chen, S.-H.; Chan, C.-H.; Lee, C.-C. Replica of the structural color for *Papilio blumei* butterfly. *J. Nanophotonics* **2013**, *7* (1), 073597.

(234) Aryal, M.; Ko, D.-H.; Tumbleston, J. R.; Gadisa, A.; Samulski, E. T.; Lopez, R. Large area nanofabrication of butterfly wing's three dimensional ultrastructures. *J. Vac. Sci. Technol., B: Nanotechnol. Microelectron.: Mater., Process., Meas., Phenom.* **2012**, *30* (6), 061802.

(235) Franz, S.; Rammelt, S.; Scharnweber, D.; Simon, J. C. Immune responses to implants – A review of the implications for the design of immunomodulatory biomaterials. *Biomaterials* **2011**, *32* (28), 6692–6709.

(236) Anderson, J. M.; Rodriguez, A.; Chang, D. T. Foreign body reaction to biomaterials. *Semin. Immunol.* **2008**, *20* (2), 86–100.

(237) Saito, A.; Yoshioka, S.-y.; Kinoshita, S. Reproduction of the Morpho butterfly's blue: arbitration of contradicting factors. *Proc. SPIE* **2004**, *5526*, 188–195.

(238) Watanabe, K.; Hoshino, T.; Kanda, K.; Haruyama, Y.; Matsui, S. Brilliant blue observation from a Morpho-butterfly-scale quasi-structure. *Jpn. J. Appl. Phys.* **2005**, *44* (1L), L48.

(239) Martín-Palma, R. J.; Pantano, C. G.; Lakhtakia, A. Biomimetization of butterfly wings by the conformal-evaporated-film-by-rotation technique for photonics. *Appl. Phys. Lett.* **2008**, *93* (8), 083901.

(240) Crne, M.; Sharma, V.; Blair, J.; Park, J. O.; Summers, C. J.; Srinivasarao, M. Biomimicry of optical microstructures of *Papilio palinurus*. *EPL* **2011**, *93* (1), 14001.

(241) Bao, X.; Bontemps, A.; Grondel, S.; Cattan, E. Design and fabrication of insect-inspired composite wings for MAV application using MEMS technology. *J. Micromech. Microeng.* **2011**, *21* (12), 125020.

(242) Pris, A. D.; Utturkar, Y.; Surman, C.; Morris, W. G.; Vert, A.; Zalyubovskiy, S.; Deng, T.; Ghiradella, H. T.; Potyrailo, R. A. Towards high-speed imaging of infrared photons with bio-inspired nanoarchitectures. *Nat. Photonics* **2012**, *6* (3), 195–200.

(243) Siddique, R. H.; Diewald, S.; Leuthold, J.; Hölscher, H. Theoretical and experimental analysis of the structural pattern responsible for the iridescence of Morpho butterflies. *Opt. Express* **2013**, *21* (12), 14351–14361.

(244) Miyako, E.; Sugino, T.; Okazaki, T.; Bianco, A.; Yudasaka, M.; Iijima, S. Self-assembled carbon nanotube honeycomb networks using a butterfly wing template as a multifunctional nanobiohybrid. *ACS Nano* **2013**, *7* (10), 8736–8742.

(245) Song, B.; Eom, S. C.; Shin, J. H. Disorder and broad-angle iridescence from Morpho-inspired structures. *Opt. Express* **2014**, *22* (16), 19386–400.

(246) Poncelet, O.; Tallier, G.; Simonis, P.; Cornet, A.; Francis, L. A. Synthesis of bio-inspired multilayer polarizers and their application to anti-counterfeiting. *Bioinspiration Biomimetics* **2015**, *10* (2), 026004.

(247) Chen, Y.-C.; Huang, Z.-S.; Yang, H. Cicada-wing-inspired Self-cleaning antireflection coatings on polymer substrates. *ACS Appl. Mater. Interfaces* **2015**, *7* (45), 25495–25505.

(248) Huang, Y.-F.; Jen, Y.-J.; Chen, L.-C.; Chen, K.-H.; Chattopadhyay, S. Design for approaching cicada-wing reflectance in low-and high-index biomimetic nanostructures. *ACS Nano* **2015**, *9* (1), 301–311.

(249) Liu, Y.; Song, Y.; Niu, S.; Zhang, Y.; Han, Z.; Ren, L. Integrated super-hydrophobic and antireflective PDMS bio-templated from nano-conical structures of cicada wings. *RSC Adv.* **2016**, *6* (110), 108974–108980.

(250) Gan, Z.; Turner, M. D.; Gu, M. Biomimetic gyroid nanostructures exceeding their natural origins. *Sci. Adv.* **2016**, *2* (5), No. e1600084.

(251) Fraioli, R.; Tsimbouri, P. M.; Fisher, L. E.; Nobbs, A. H.; Su, B.; Neubauer, S.; Rechenmacher, F.; Kessler, H.; Ginebra, M.-P.; Dalby, M. J.; Manero, J. M.; Mas-Moruno, C. Towards the cell-instructive bactericidal substrate: exploring the combination of nanotopographical features and integrin selective synthetic ligands. *Sci. Rep.* **2017**, *7* (1), 16363.

(252) Ahmed, R.; Ji, X.; Atta, R. M. H.; Rifat, A. A.; Butt, H. Morpho butterfly-inspired optical diffraction, diffusion, and bio-chemical sensing. *RSC Adv.* **2018**, *8* (48), 27111–27118.

(253) Fang, Y.; Sun, G.; Bi, Y.; Zhi, H. Multiple-dimensional micro/nano structural models for hydrophobicity of butterfly wing surfaces and coupling mechanism. *Sci. Bull.* **2015**, *60* (2), 256–263.

(254) Hu, H.-M.; Watson, J. A.; Cribb, B. W.; Watson, G. S. Fouling of nanostructured insect cuticle: adhesion of natural and artificial contaminants. *Biofouling* **2011**, *27* (10), 1125–1137.

(255) Liu, G.; Dong, H.; Li, C. Vortex dynamics and new lift enhancement mechanism of wing–body interaction in insect forward flight. *J. Fluid Mech.* **2016**, *795*, 634–651.